

Multidimensional Scaling of Noisy High Dimensional Data

Erez Peterfreund^{1,*}, Matan Gavish^{1,**}

The Hebrew University of Jerusalem

Abstract

Multidimensional Scaling (MDS) is a classical technique for embedding data in low dimensions, still in widespread use today. Originally introduced in the 1950's, MDS was not designed with high-dimensional data in mind; while it remains popular with data analysis practitioners, no doubt it should be adapted to the high-dimensional data regime. In this paper we study MDS under modern setting, and specifically, high dimensions and ambient measurement noise. We show that, as the ambient noise level increase, MDS suffers a sharp breakdown that depends on the data dimension and noise level, and derive an explicit formula for this breakdown point in the case of white noise. We then introduce MDS+, an extremely simple variant of MDS, which applies a carefully derived shrinkage nonlinearity to the eigenvalues of the MDS similarity matrix. Under a loss function measuring the embedding quality, MDS+ is the unique asymptotically optimal shrinkage function. We prove that MDS+ offers improved embedding, sometimes significantly so, compared with classical MDS. Furthermore, MDS+ does not require external estimates of the embedding dimension (a famous difficulty in classical MDS), as it calculates the optimal dimension into which the data should be embedded.

Keywords: Multidimensional scaling, Euclidean embedding, dimensionality reduction, singular value thresholding, optimal shrinkage, MDS+

1. Introduction

Manifold learning and metric learning methods have become central items in the toolbox of any modern data scientist. These techniques seek to reconstruct a global, low-dimensional geometric structure of a dataset from pairwise similarity measurements [1, 2, 3, 4, 5, 6, 7].

Multidimensional Scaling [8] (MDS) was the first metric learning algorithm proposed, and arguably the one most widely used today. It is used extensively for exploratory data analysis, inference and visualization in many science and engineering disciplines, as well as in psychology, medicine and the social sciences [9, 10, 11, 12, 13].

In the MDS algorithm, one considers an unknown point cloud $\mathbf{b}_1, \dots, \mathbf{b}_n \in \mathbb{R}^p$ and assumes that only the distances $\Delta_{i,j} = \|\mathbf{b}_i - \mathbf{b}_j\|^2$ are observable. MDS, which aims to reconstruct the global spatial configuration of the point cloud, proceeds as follows.

*corresponding author: erezpeter@cs.huji.ac.il

**corresponding author: gavish@cs.huji.ac.il

¹School of Computer Science and Engineering, The Hebrew University, Jerusalem, Israel

1. First, form the similarity matrix

$$S = -\frac{1}{2}H \cdot \Delta \cdot H, \quad (1)$$

where $H = I - \frac{1}{n}\mathbf{1} \cdot \mathbf{1}^\top$ is a data-centering matrix.

2. Next, diagonalize S to form

$$S = U \cdot D \cdot U' \quad (2)$$

where $D = \text{diag}(d_1, \dots, d_n)$ and U is orthogonal with orthonormal columns $\mathbf{u}_1, \dots, \mathbf{u}_n$.

3. Then, estimate (or guess) the original dimension of the point cloud, $r = \dim \text{Span}\{\mathbf{b}_1, \dots, \mathbf{b}_n\}$.
4. Finally, return the n -by- r matrix with columns $\sqrt{d_i} \cdot \mathbf{u}_i$ ($i = 1, \dots, r$). Embed the points into \mathbb{R}^r using the rows of this matrix.

This paper addresses two crucial issues that remain open in the practice of MDS on high-dimensional data: the effect of ambient noise, and the choice of embedding dimension. As we will see, while these issues are seemingly different, they are in fact very closely related. Let us first elaborate on each issue in turn.

1.1. Choice of embedding dimension

While MDS is extremely popular among practitioners in all walks of science, there is a decades-old inherent conundrum involved in its use in practice. Strangely, the literature offers no systematic method for choosing the embedding dimension r . The original paper [8], as well as numerous authors since, have proposed various heuristics for choosing the “correct” embedding dimension. In fact, recent tutorials such as [14], and even the SPSS user’s manual², still offer no systematic method and recommend Cattell’s *Scree Plot* heuristic [15], a 50-year-old method based on subjective visual inspection of the data.

Our first main contribution in this paper is a systematic method for choosing r , the embedding dimension, from the data. The estimator \hat{r} we propose is provably optimal in the asymptotic regime $n, p \rightarrow \infty$, under a suitable loss function quantifying the embedding quality, and under the assumption of white ambient noise.

Concretely, Table 1 shows the value of the optimal hard threshold λ^* for MDS, a concept we develop below. To find the asymptotically optimal embedding dimension \hat{r} in an MDS problem with n vectors in ambient dimension p and white ambient noise with standard deviation σ , simply proceed as follows. First, let $\beta = (n - 1)/p$ and find the value λ^* from Table 1 (Python and Matlab code to evaluate λ^* exactly is provided in the code supplement [16], based on formula (24) below). Then, let \hat{r} be the number of eigenvalues the matrix S from (1) that fall above the threshold $(\sigma \cdot \lambda^*)^2$. If σ is unknown, as is often the case, use the consistent and robust estimator $\hat{\sigma}$ from (29) below instead; an implementation of this estimator is included in the code supplement [16].

²https://www.ibm.com/support/knowledgecenter/SSLVMB_23.0.0/spss/tutorials/proxscal_data_howto.html. (Accessed 1/1/2018)

β	0.05	0.1	0.15	0.2	0.25	0.3	0.35	0.4	0.45	5
λ^*	1.301	1.393	1.467	1.531	1.588	1.639	1.688	1.733	1.775	1.816

β	0.55	0.6	0.65	0.7	0.75	0.8	0.85	0.9	0.95	1
λ^*	1.854	1.891	1.927	1.962	1.995	2.028	2.059	2.09	2.12	2.149

Table 1: The optimal threshold for MDS - see Section 3 below. The asymptotically optimal embedding dimension \hat{r} is obtained by counting the eigenvalues of the matrix S from (1) that fall above the threshold $(\sigma\lambda^*)^2$. If σ is unknown, as is often the case, use the consistent and robust estimator $\hat{\sigma}$ from (29).

1.2. Breakdown of MDS in high-dimensional ambient noise

In the six decades since MDS was proposed, typical datasets have grown in both size and dimension. MDS, as well as more recently proposed manifold learning techniques, are being applied to data of increasingly high ambient dimensions, departing from the setup $p \ll n$ for which they were originally designed. In particular, when the data is high-dimensional, certain mathematical phenomena kick in, which fundamentally alter the behavior of MDS.

In practice, even though the data is measured in an ambient high dimensional space, it often resides on a low-dimensional structure embedded in that space. Manifold learning techniques, for example, assume that the data resides on a low-dimensional smooth manifold embedded in the high-dimensional space. For simplicity, consider an “original” dataset $\{\mathbf{a}_1, \dots, \mathbf{a}_n\} \subset \mathbb{R}^d$ that resides on a d -dimensional linear subspace ($d \ll p$), embedded in the ambient space \mathbb{R}^p , in which the data is actually measured. It is natural to assume that the measurements are noisy, so that we actually observe samples b_1, \dots, b_n with

$$b_i = \rho(\mathbf{a}_i) + \varepsilon_i \quad i = 1, \dots, n,$$

where $\rho : \mathbb{R}^d \hookrightarrow \mathbb{R}^p$ is the isometry embedding the low-dimensional subspace into the ambient space, and where $\varepsilon_i \in \mathbb{R}^p$ are ambient noise vectors ($i = 1, \dots, n$).

When the ambient dimension p is not much smaller than the sample size n , the presence of ambient noise can have drastic effects on the diagonalization step of MDS. In particular, in the related scenario of covariance matrix estimation, results from high dimensional statistics [17] and random matrix theory [18] have shown in that the eigenvalues and eigenvectors of the data matrix deviate, sometimes significantly, from the embedding vectors they are presumed to estimate. As a result, the quality of the MDS embedding becomes sensitive to the ambient noise level. In this paper we demonstrate that a phenomenon names after Baik, Ben-Arous and P  ch   [18] occurs in MDS, whereby there is a sharp phase transition in the embedding quality (see examples in Section 1.4 below, Figure 3 and Figure 4).

Our second main contribution is formal characterization of this phenomenon in MDS. We show that, as the ambient noise level increases, MDS suffers a sharp *breakdown*, and provide an asymptotically exact formula for the signal-to-noise level at which breakdown occurs.

1.3. An optimal variant of MDS

Even before breakdown occurs, in the high-dimensional setting, the quality of the MDS embedding deteriorates as the ambient noise level increases. This calls for an improvement of MDS, which is able to correct for the noise effects. Experience tells us that complicated alternatives of

MDS do not become widely used by scientists. Instead, a simple variation on MDS is preferred, which can be calculated easily based on the existing MDS methodology.

A simple solution is available in the form of *eigenvalue shrinkage*. Recently, in the related problem of covariance matrix estimation, [19] have shown that, by applying a carefully designed shrinkage function to the eigenvalues of a sample covariance matrix, it is possible to significantly mitigate the effects of high-dimensional ambient noise.

Here, we consider a simple variant of MDS that applies a univariate shrinkage function $\eta : \mathbb{R} \rightarrow \mathbb{R}$ to the eigenvalues d_1, \dots, d_n of the MDS matrix S from (1). Instead of using the eigenvalues d_1, \dots, d_n of S as in (2) above, we use the shrunken values $\eta(\sqrt{d_1}), \dots, \eta(\sqrt{d_n})$ – see example in Section 1.4 below, Figure 5 and Figure 6. In fact, classical MDS turns out to be equivalent to a specific choice of hard threshold shrinker. The question naturally arises whether better shrinkers can be designed, which outperform classical MDS.

The third main contribution of this paper is MDS+, formally defined in Table 2 below. MDS+ is a simple variant of MDS which applies a carefully derived shrinkage function to the eigenvalues d_1, \dots, d_n before proceeding with the MDS embedding.

Concretely, MDS+ is a simple modification of MDS: In step 4 above, instead of the MDS embedding that uses $\sqrt{d_i} \cdot \mathbf{u}_i$ we embed using $\eta^*(\sqrt{d_i}) \cdot \mathbf{u}_i$, where η^* is the *optimal shrinker* for MDS:

$$\eta^*(y) = \begin{cases} \sigma \sqrt{(x(y)/\sigma)^2 - \beta - \frac{\beta \cdot (1-\beta)}{(x(y)/\sigma)^2 + \beta}} & y > \sigma \cdot (1 + \sqrt{\beta}) \\ 0 & \text{otherwise} \end{cases}$$

where

$$x(y) = \frac{\sigma}{\sqrt{2}} \sqrt{\left(\frac{y}{\sigma}\right)^2 - 1 - \beta + \sqrt{\left(\left(\frac{y}{\sigma}\right)^2 - 1 - \beta\right)^2 - 4\beta}}.$$

Here, as above, $\beta = (n - 1)/p$ and σ is the standard deviation of the noise, replaced by the consistent robust estimate $\hat{\sigma}$ from (29) in case σ is unknown.

Figure 1 below compares the optimal shrinker underlying MDS+ with the hard threshold shrinker underlying classical MDS.

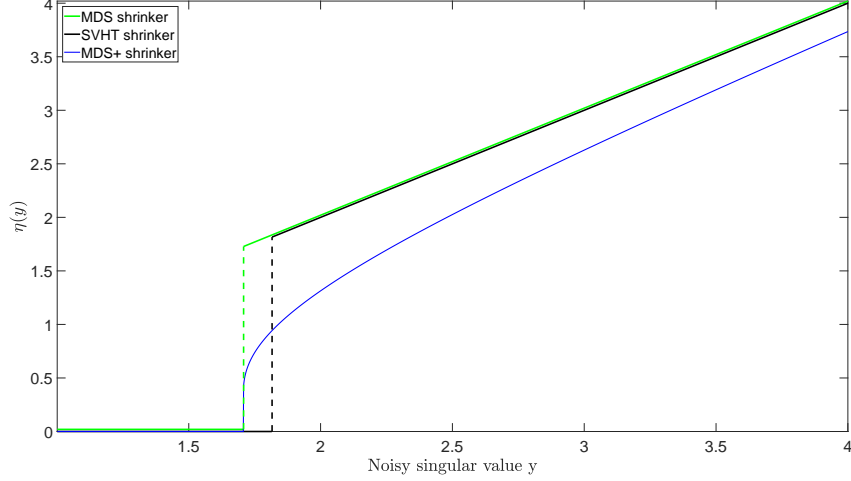


Figure 1: The optimal shrinker derived in this paper, compared with an optimal hard threshold SVHT (see below) and the classical MDS shrinker. Specific parameters are used – see figure 7 and section 3. (Color online)

As the figure shows, if $\sqrt{d_i}$ is too small, and specifically if $d_i \leq \sigma \cdot (1 + \sqrt{\beta})$, $\eta^*(\sqrt{d_i}) = 0$. In this case the vector \mathbf{u}_i is not used in the embedding, resulting in a smaller embedding dimension. In other words, the embedding dimension used by MDS+ equals the amount of eigenvalues of the matrix S that fall above the value $\sigma^2 \cdot (1 + \sqrt{\beta})^2$. Table 2 below summarizes the MDS+ algorithm.

Measuring the embedding quality using a natural loss function, we prove that MDS+ offers the *best possible embedding*, asymptotically, among any eigenvalue shrinkage variant of MDS.

MDS+

Input: distance matrix Δ and dimensionality p .

Let $\beta = (n - 1)/p$. Let the value of σ be given or estimated (see Theorem 6 below).

1. Create the similarity matrix

$$S = -\frac{1}{2}H \cdot \Delta \cdot H$$

2. Diagonalize S to obtain

$$S = U \cdot D \cdot U'$$

where $U \in O(n)$ and $D = \text{diag}(d_1, \dots, d_n)$ s.t. $d_1 \geq \dots \geq d_n$.

3. Estimate the embedding dimension

$$r = \#\{i \in \{1, \dots, n\} : d_i > \sigma \cdot (1 + \sqrt{\beta})\}.$$

4. Return a n -by- r matrix with columns $\eta^*(\sqrt{d_i}) \cdot \mathbf{u}_i$ ($i = 1, \dots, r$),

where η^* is as in Theorem 3. Embed the points into \mathbb{R}^r using the rows of the matrix.

Table 2: The MDS+ Algorithm

1.4. Examples

As a gentle introduction to our results, we consider two simple examples of MDS from noisy, high-dimensional data.

MNIST. The famous MNIST dataset [20] contains greyscale images of hand-written digits. Clustering after MDS embedding (a form of spectral clustering) is often used to distinguish between different digits. For illustration purposes, we studied 700 images of the digits 0 and 1 (Figure 2), with varying levels of added white Gaussian noise. As the data consists of two distinct clusters, it should be enough to use MDS embedding into $r = 2$ dimensions. Figure 3 clearly shows the deteriorating embedding quality as the noise level increases, and the eventual MDS breakdown, accurately predicted by Theorem 1 below.



Figure 2: Example of images from MNIST [20]

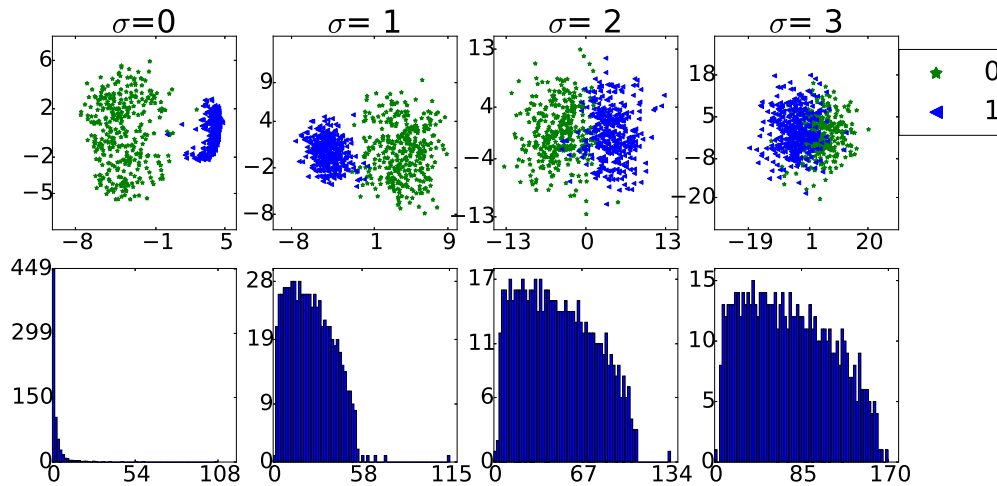


Figure 3: Breakdown of MDS on MNIST data. $n = 700$ images in $p = 784$ dimensions (pixels). Gaussian i.i.d noise $N(0, \sigma^2)$ added as indicated in each column. Top panels: MDS embedding into $r = 2$ dimensions. Bottom panels: histogram of the corresponding square root of the spectra of the MDS matrix S from (1). Observe that breakdown occurs exactly as the noise-related eigenvalues, which grow proportionally to σ , “engulf” the lowest structure-related eigenvalue. (Color online)

Helix. A recent application of MDS in molecular biology is analysis of Hi-C measurements [21]. Here, MDS is used to recover the three-dimensional packing of DNA molecules inside the cell nucleus from measurements of spatial affinity between loci along the genome. As a toy example for this reconstruction problem, we consider a reconstruction of a helix-shaped point cloud in \mathbb{R}^3 from the pairwise distances between $n = 300$ points in the cloud. The point cloud was embedded

in a high dimensional space \mathbb{R}^{500} , and i.i.d Gaussian ambient noise of a varying level was added. Figure 4 demonstrates the deterioration of MDS embedding quality with increasing noise level, and the corresponding spectra of the MDS matrix.

Figure 5 demonstrates the effect of the improved MDS algorithm we propose, based on optimal shrinkage of the MDS eigenvalues. The breakdown of MDS is apparent in the right panel. The optimal shrinker identifies that one of the MDS axes is non-informative, and shrinks the corresponding eigenvalue to zero. As a result, the MDS+ embedding is two-dimensional (Figure 6).

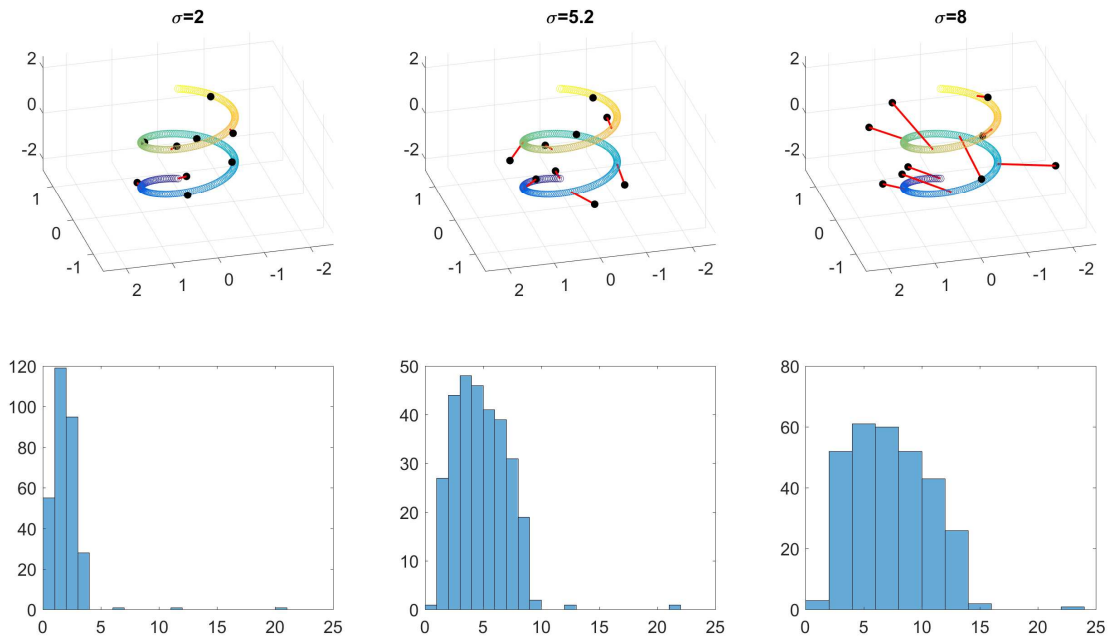


Figure 4: Breakdown of MDS on a helix simulation. $n = 300$ points along a helix embedded in $p = 500$ dimensions. Gaussian i.i.d noise $\mathcal{N}(0, \sigma^2)$ was added as indicated in each column. Top panels: MDS embedding into $r = 3$ dimensions (solid: original helix shape. black markers: some points of the embedded data. red lines: displacement vectors between the embedding and real position of the data). Bottom panels: histogram of the corresponding square root of the spectra of the MDS matrix S from (1). Observe that breakdown occurs exactly as the noise-related eigenvalues, which grow proportionally to σ , “engulf” the lowest structure-related eigenvalue. (Color online)

1.5. Related work

Classical MDS. Precursors of MDS go back as far as 1938 to Young and Householder’s work on Classical Scaling algorithm [22]. The MDS algorithm as we know it today has been developed by several authors, notably Torgerson [9] and Gower [23].

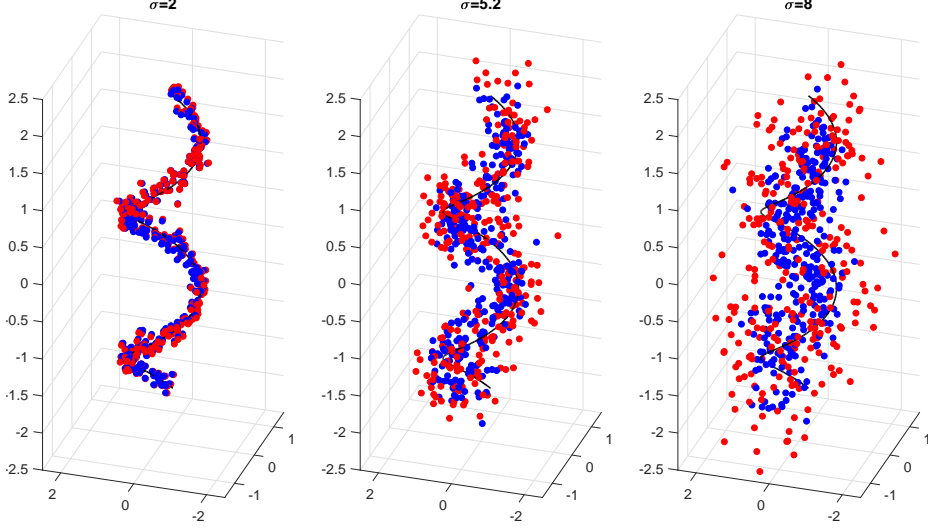


Figure 5: The MDS+ algorithm on the helix simulation from Figure 4. Red: classical MDS. Blue: MDS+. An additional view of the right panel is available in Figure 6 below. (Color online)

Choosing the embedding dimension. Classical choice of embedding dimension is based on the fact that the similarity matrix (1) should be positive semidefinite.

The literature offers two popular heuristics for choosing the embedding dimension that are based on this fact. In the *Scree Plot* method [15] one plots the eigenvalues (d_1, \dots, d_n) from (2) in decreasing order over $(1, \dots, n)$, and looks for the “inflection”, “knee” or “elbow” in the plot to determine r . The rationale behind this visual heuristic is that the “scree”, namely the slowly changing eigenvalues (below the inflection point) are due to the noise, while the top eigenvalues (above the inflection point) are due to the d -dimensional subspace containing the signal. In a different heuristic for choosing r , one seeks to maximize the function

$$\frac{\sum_{i=1}^r d_i}{\sum_{i=1}^{\text{rank}(S)} d_i} \quad (3)$$

while keeping the selected embedding dimension r as low as possible [24].

In some cases the actual distance matrix gets corrupted, and as a result the similarity matrix may have one or more negative eigenvalues. In this case it is commonly suggested to choose the embedding dimension by maximizing one of the following target functions [11]:

$$\frac{\sum_{i=1}^r \lambda_i}{\sum_{i=1}^{\text{rank}(S)} |\lambda_i|} \quad \text{or} \quad \frac{\sum_{i=1}^r \lambda_i}{\sum_{i=1}^{\text{rank}(S)} \max(0, \lambda_i)} \quad (4)$$

In another heuristic for choosing r , due to Kruskal [25], one considers the so-called *Stress-1* function:

$$\sigma_1 = \sqrt{\frac{\sum_{i,j} (\Delta_{i,j} - \hat{\Delta}_{i,j})^2}{\sum_{i,j} (\Delta_{i,j})^2}} \quad (5)$$

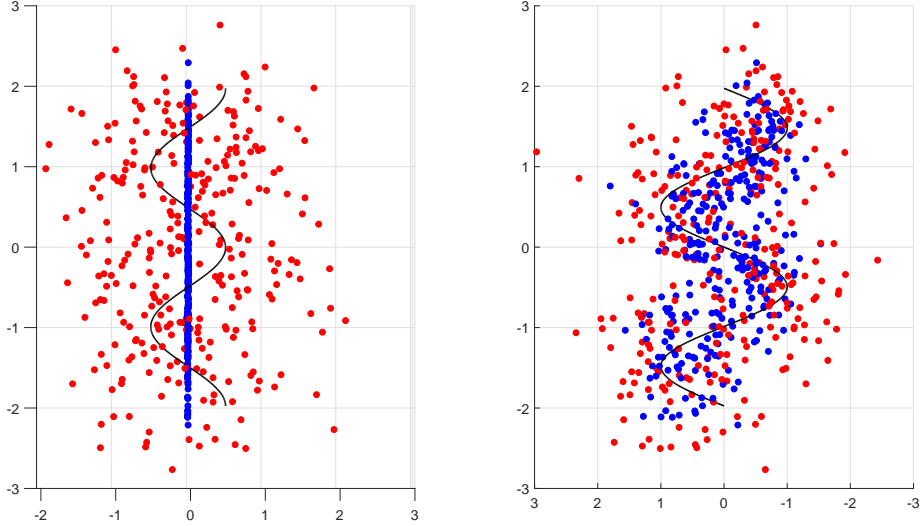


Figure 6: The MDS+ algorithm on the helix simulation from Figure 4 in high noise, $\sigma = 8$. Red: classical MDS. Blue: MDS+. Embedding into \mathbb{R}^3 spanned by the standard basis vectors e_1, e_2, e_3 . Left: the (e_2, e_3) plane. Right: the (e_1, e_3) plane. (Color online)

where $\hat{\Delta}_{i,j}$ is the euclidean distance between the embedding of point i and the embedding of point j . Kruskal proposed to choose the embedding dimension r by minimizing σ_1 .

One striking observation regarding the selection of embedding dimension is that even though MDS and its variants are extremely popular, the literature does not propose a systematic method that is backed up by rigorous theory.

Algorithm performance in the presence of noise. To the best of our knowledge, the literature does not offer a systematic treatment on the influence of ambient noise on MDS embedding quality. Kruskal’s variation of MDS [26] was studied by Cox and Cox [27], who have shown by simulation that the stress function is an almost perfectly linear function of the noise when $d = r = 2$, independently of the amount of samples.

1.6. Outline

This paper proceeds as follows. In Section 2 we provide the formal problem setup, and propose a loss function to quantify the quality of any low-dimensional embedding algorithm. Our main results are stated in Section 3 and discussed in Section 4. The proofs appear in Section 5, where we also show how to estimate the ambient noise level. While our main results are stated under the assumption $n - 1 \leq p$, in the Appendix we rigorously extend our results to the case $n - 1 \geq p$.

1.7. Reproducibility Advisory

The algorithms developed in this paper have been implemented in both Python and Matlab and are made available in the code supplement [16]. The code supplement also includes source code to reproduce all the figures in this paper.

2. Problem setup

2.1. Notation

Let $a_+ = \max(a, 0)$ denote the positive part of $a \in \mathbb{R}$. We use boldface letters such as $\mathbf{b} \in \mathbb{R}^p$ to denote a vector with coordinates $[(\mathbf{b})_1, \dots, (\mathbf{b})_p]$ and Euclidean norm $\|\mathbf{b}\|_2$. We use capital letters such as A to denote a matrix with transpose A^\top . The i -th column and j -th row of A will be denoted by $A_{*,i}$ and $A_{j,*}$ respectively. Denote the set of m -by- n real matrices by $M_{m \times n}$ and the set of orthogonal matrices by $O(n) \subset M_{n \times n}$. The Frobenius norm of $A \in M_{m \times n}$ is defined by

$$\|A\|_F = \sqrt{\sum_{i=1}^m \sum_{j=1}^n A_{i,j}^2}.$$

Let $\mathbf{1}_p \in \mathbb{R}^p$ denote the vector $\mathbf{1}_p = (1, \dots, 1)$ and let $\mathbf{1}_{m \times n}$ denote the ‘‘all-ones’’ m -by- n matrix $\mathbf{1}_{m \times n} = \mathbf{1}_m \mathbf{1}_n^\top$. Similarly, let $\mathbf{0}_p \in \mathbb{R}^p$ denote the vector $\mathbf{0}_p = (0, \dots, 0)$ and let $\mathbf{0}_{m \times n}$ denote the ‘‘all-zeros’’ m -by- n matrix. For some d_1, \dots, d_n we denote by $\text{diag}(d_1, \dots, d_n)$ the n -by- n diagonal matrix with main diagonal d_1, \dots, d_n . The n -by- n identity matrix $\text{diag}(1, \dots, 1)$ is denoted by I_n . We also denote the m -by- n ‘‘all-zeros’’ matrix, with ones only on its main diagonal using $I_{m \times n}$. Finally, we use H to denote the MDS centralization matrix

$$H = I_n - \frac{1}{n} \mathbf{1} \cdot \mathbf{1}^\top = I_n - \frac{1}{n} \mathbf{1}_{n \times n}. \quad (6)$$

2.2. Setup

In this paper we consider MDS and its variants when applied to noisy, high dimensional measurements of a dataset with low intrinsic dimension. Let d denote the (low) intrinsic dimension and assume that we are interested in the unknown, unobservable dataset $\{\mathbf{a}_i\}_{i=1}^n \subset \mathbb{R}^d$. These data are embedded in a high dimensional space \mathbb{R}^p via an unknown rotation matrix $R \in O(p)$, such that

$$\tilde{\mathbf{a}}_i = R \cdot \begin{pmatrix} \mathbf{a}_i \\ \mathbf{0}_{p-d} \end{pmatrix} \quad i = 1, \dots, n. \quad (7)$$

However, we only observe a noisy version of the embedded dataset, which we denote by $\{\mathbf{b}_i\}_{i=1}^n \subset \mathbb{R}^p$. Formally,

$$\mathbf{b}_i = \tilde{\mathbf{a}}_i + \varepsilon_i \quad i = 1, \dots, n \quad (8)$$

where $\{\varepsilon_i\}_{i=1}^n \stackrel{iid}{\sim} \mathcal{N}_p(\mathbf{0}_p, \frac{\sigma}{\sqrt{p}} \cdot I_p)$ is ambient noise of level σ . (Note that in the introduction we used noise level without normalization; henceforth noise level σ implies noise standard deviation σ/\sqrt{p} .) While we assume $d < n \leq p$, we will focus on the regime $d \ll n$ and $n \sim p$. The assumption $n - 1 \leq p$ helps simplify results and proofs; the case $n - 1 \geq p$ is discussed in the Appendix.

It is convenient to stack the data vectors as rows and form the data matrices $X \in \mathbb{R}^{n \times d}$ and $Y \in \mathbb{R}^{n \times p}$ such that

$$X_{i,*} = \mathbf{a}_i^\top \quad i = 1, \dots, n \quad (9)$$

$$Y_{i,*} = \mathbf{b}_i^\top \quad i = 1, \dots, n. \quad (10)$$

Observe that both X (resp. Y) is a multivariate data matrix with n rows, or samples, and d (resp. p) columns, or features. we define the aspect ratio of the matrix Y as $\beta = (n - 1)/p$.

For simplicity, we will assume that the data $\{\mathbf{a}_i\}_{i=1}^n$ is centered around the origin, meaning that $H \cdot X = X$. Denote the singular values of the n -by- d matrix X by $x_1 \geq \dots \geq x_d \geq 0$ and the singular values of the n -by- p matrix $H \cdot Y$ by $y_1 \geq \dots \geq y_n \geq 0$.

2.3. The classical MDS algorithm

The classical MDS algorithm, described briefly in the introduction, is provided with two arguments. The first is $\Delta \in M_{n \times n}$, a matrix that contains the pairwise distances over the observable data, $\Delta_{i,j} = \|b_i - b_j\|_F^2$. The second is r , the dimension into which the data is to be embedded. An equivalent formal description of classical MDS consists of the two following steps:

1. Define the similarity matrix

$$S = -\frac{1}{2}H \cdot \Delta \cdot H \quad (11)$$

2. Find a n -by- r matrix \hat{X} by

$$\hat{X}^{MDS} = \underset{Z \in M_{n \times r}: \tilde{V}_Z = I}{\operatorname{argmin}} \|S - Z \cdot Z^\top\|_F^2, \quad (12)$$

where \tilde{V}_Z is the right singular vector matrix of Z , and use the rows of \hat{X} to embed the n data points in \mathbb{R}^r . In other words, we optimize over matrices $Z \in M_{n \times r}$ such that $Z^\top Z$ is diagonal. Note that $\hat{X}_{i,*}$ is the embedding coordinates of i -th datapoint. While \hat{X} depends on r , we leave this dependency implicit in the notation. Being the number of columns of \hat{X} , it is easy to infer from context.

It is easy to verify that the MDS algorithm mentioned in section 1 is equivalent to the one above. In fact, the MDS admits a more convenient formulation, as follows. Theorem 7 below states that $S = (HY) \cdot (HY)^\top$. As a result, we have the following lemma.

Lemma 1. *Let $S \in M_{n \times n}$ be a similarity matrix as in (11). Then for any $i = 1, \dots, \operatorname{rank}(S)$ we have*

1. $\sqrt{d_i} = y_i$, where d_i is the i -th eigenvalue of S .
2. There exists $q \in \{\pm 1\}$ such that

$$\mathbf{u}_i = q \cdot \mathbf{w}_i$$

where \mathbf{u}_i is the i -th left singular value of $H \cdot Y$ and \mathbf{w}_i is the i -th eigenvector of S .

It follows that the MDS embedding (12) is given equivalently by

$$\hat{X}^{MDS} = \sum_{i=1}^r y_i q_i \mathbf{u}_i \mathbf{e}_i^\top \quad (13)$$

where $\mathbf{e}_i \in \mathbb{R}^r$ are the standard basis vectors and $q_1, \dots, q_r \in \{\pm 1\}$.

2.4. Formal analysis of MDS accuracy

MDS was originally developed for the noiseless scenario. Indeed, when no noise is present, if the parameter r provided equals to the latent dimension d , it is well known that

$$\hat{X}_{i,*}^\top = R \cdot \mathbf{a}_i \quad i = 1, \dots, n \quad (14)$$

for some $R \in O(d)$. In other words, in the absence of noise, if $r = d$, MDS recovers the latent (low-dimensional) data vectors $\mathbf{a}_1, \dots, \mathbf{a}_n$ exactly - up to a global rotation. A proof of this fact is provided in Section 5, see Theorem 8.

Clearly, in the presence of noise ($\sigma > 0$) one cannot hope for exact recovery, and some formal measure of ‘‘MDS accuracy’’ is required. Such a notion of accuracy is traditionally obtained by introducing a loss function. Consider the following loss function, which measures the ‘‘proximity’’ of the point cloud recovered by MDS to the original, unknown point cloud that MDS aims to recover.

Definition 1 (Similarity distance). *Given two datasets $\{\mathbf{a}_i\}_{i=1}^n \subset \mathbb{R}^d$, $\{\mathbf{b}_i\}_{i=1}^n \subset \mathbb{R}^r$, where $d, r \in \mathbb{N}$, define a generic distance between the two datasets by*

$$M_n(\{\mathbf{a}_i\}_{i=1}^n, \{\mathbf{b}_i\}_{i=1}^n) = \min_{R \in O(l)} \sum_{i=1}^n \left\| \begin{bmatrix} \mathbf{a}_i - \frac{1}{n} \sum_{i=1}^n \mathbf{a}_i \\ \mathbf{0}_{l-d} \end{bmatrix} - R \cdot \begin{bmatrix} \mathbf{b}_i - \frac{1}{n} \sum_{i=1}^n \mathbf{b}_i \\ \mathbf{0}_{l-d} \end{bmatrix} \right\|_2$$

where $l = \max(d, r)$.

Observe that using our matrix notation this formula could be written as

$$M_n(\{\mathbf{a}_i\}_{i=1}^n, \{\mathbf{b}_i\}_{i=1}^n) = \min_{R \in O(l)} \left\| H \cdot [A, \mathbf{0}_n \times (l-d)^+] - H \cdot [B, \mathbf{0}_n \times (l-d)^+] \cdot R \right\|_2.$$

Here, $A \in M_{n \times d}$ is a column stacking of the $\{a_i\}$, namely $A_{i,*} = a_i^\top$. Similarly $B \in M_{n \times r}$ is a column stacking of $\{b_i\}$.

While the function M_n depends on (n, d, r) , we suppress d and r in the notation M_n and leave them to be inferred from context. We first observe that in the noiseless case, classical MDS does indeed find the minimum of this loss function:

Lemma 2. *Let $\sigma = 0$, let $n \in \mathbb{N}$ be arbitrary and let $d < n$. Then for any $r \geq d$, the MDS solution from (12) with embedding dimension r satisfies*

$$\hat{X}^{MDS} \in \underset{A \in M_{n \times r}}{\operatorname{argmin}} M_n(A, X) \quad (15)$$

Moreover, $M_n(\hat{X}^{MDS}, X) = 0$.

It follows that an algorithm that tries to minimize $M_n(\cdot, X)$ will agree with classical MDS in the noiseless case. We now argue that M_n is a natural loss for measuring the MDS accuracy in the noisy case as well. Observe that a reasonable loss for measuring MDS accuracy must satisfy the following properties:

1. *Rotation invariance.* We say that a loss M_n is rotation-invariant if

$$M_n(Y_1, Y_2 \cdot R) = M_n(Y_1, Y_2) \quad (16)$$

for any two data matrices $Y_1, Y_2 \in M_{n \times p}$ and any rotation matrix $R \in O(p)$.

2. *Translation invariance.* We say that a loss M_n is translation-invariant if

$$M_n \left(Y_1, Y_2 + \begin{bmatrix} \mathbf{c}^T \\ \mathbf{c}^T \\ \dots \\ \mathbf{c}^T \end{bmatrix} \right) = M_n(Y_1, Y_2) \quad (17)$$

for any two data matrices $Y_1, Y_2 \in M_{n \times p}$ and any translation vector $\mathbf{c} \in \mathbb{R}^p$.

3. *Padding invariance.* We say that a loss M_n is padding-invariant if

$$M_n \left(\begin{bmatrix} Y_1 & \begin{bmatrix} \mathbf{c}^T \\ \mathbf{c}^T \\ \dots \\ \mathbf{c}^T \end{bmatrix} \end{bmatrix}, Y_2 \right) = M_n(Y_1, Y_2) \quad (18)$$

for any $k \in \mathbb{N}$, $Y_1 \in M_{n \times p}$, $Y_2 \in M_{n \times (p+k)}$ and $\mathbf{c} \in \mathbb{R}^k$.

We now show that the loss M_n from Definition 1 satisfies all these invariance properties.

Lemma 3. *Let n, d and r be such that $n > r$ and $n > d$. Then the function $M_n : M_{n \times r} \times M_{n \times d} \rightarrow \mathbb{R}$ satisfies properties (1)-(3) above.*

In fact, M_n turns out to be a pseudo-metric on $M_{n \times r} \times M_{n \times d}$ when $r = d$:

Lemma 4. *Let $n \in \mathbb{N}$ and assume $r = d$. The similarity distance M_n from Definition 1 satisfies the following properties:*

1. $M_n(Y, Y) = 0$
2. $M_n(X, Y) = M_n(Y, X)$
3. $M_n(X, Y) \leq M_n(X, Z) + M_n(Z, Y)$

In summary, we arrived at the following natural definition for a loss function measuring the accuracy of MDS and MDS-type algorithms, which satisfied the fundamental properties of an embedding accuracy loss function.

Definition 2. *Let X be a dataset with n points in \mathbb{R}^d as in (9) and let Y be a noisy, high dimensional version as in (10). Let \hat{X} be an embedding in \mathbb{R}^r constructed from $H \cdot Y$, where r is an embedding dimension chosen by the scientist or the embedding algorithm used. We use the loss function*

$$L_n(\hat{X}|X) = M_n^2(\hat{X}, X)$$

to measure the accuracy of the embedding \hat{X} .

2.5. Asymptotic model

We now find ourselves in a familiar decision-theoretic setup, and familiar questions naturally arise: How does one choose an embedding algorithm with favorable loss L_n ? How does the classical MDS algorithm compare, in terms of L_n , to alternative algorithms? Is there an algorithm that achieves optimal L_n in some situations?

Unfortunately, in general, analysis of the loss function L_n is a difficult problem in the presence of ambient noise due to the complicated joint distribution of the singular values of Y_n [28, 29]. Recently, a line of works building on Johnstone's Spiked Covariance Model [30], an asymptotic

model which considers instead a sequence of increasingly larger matrices, has yielded exact forms of asymptotically optimal estimators, which were shown to be useful even in relatively small matrices in practice [31, 32, 33, 34, 35].

Following this successful approach, in this paper we consider a sequence of increasingly larger embedding problems. In the n -th problem, we observe n vectors in dimension p_n , with p growing proportionally to n . The original (low-dimensional) data matrix will be denoted $X_n \in M_{n \times d}$ (as in (9)), and the observed data matrix will be denoted $Y_n \in M_{n \times p_n}$ (as in (10)). Let $Y_n = [X_n, 0_{n \times (p-d)}] \cdot R_n + Z_n$ where $R_n \in O(p_n)$ and $Z_n, Y_n \in M_{n \times p_n}$ satisfy the following properties:

1. *Invariant white noise.* The entries of Z_n are i.i.d distributed, and drawn from a distribution with zero mean, variance σ^2/p_n , and finite fourth moment. We assume that this distribution is orthogonally invariant in the sense that for any $A \in O(n)$ and $B \in O(p_n)$ the matrix $A \cdot Z_n \cdot B$ would follow the same distribution as Z_n .
2. *Fixed signal column span* $\text{span}(x_1, \dots, x_d)$. Let $d > 0$, choose $\mathbf{x} \in \mathbb{R}^d$ with coordinates $\mathbf{x} = (x_1, \dots, x_d)$ such that $x_1 > \dots > x_d > 0$. Assume for any $n \in \mathbb{N}$

$$X_n = H \cdot X_n = U_n \cdot [\text{diag}(x_1, \dots, x_d), 0_{d \times (n-d)}]^\top \cdot \tilde{U}_n^\top \quad (19)$$

is an arbitrary singular value decomposition of X_n , where $U_n \in O(n)$ and $\tilde{U}_n \in O(d)$ are arbitrary and unknown orthogonal matrices. Additionally, we preserve the unbiased assumption on the original data.

3. *Asymptotic aspect ratio* - Let p_n be an increasing monotone sequence over \mathbb{N} , such that $\lim_{n \rightarrow \infty} (n-1)/p_n = \beta \in (0, 1]$. We consider the case $\beta \in [1, \infty)$ in the appendix section, under which we get the exact same results.

Let Δ_n be the Euclidean distance matrix on the n -th problem, so that

$$(\Delta_n)_{i,j} = \|\mathbf{b}_{i,n} - \mathbf{b}_{j,n}\|^2$$

where $\mathbf{b}_{i,n}$ is the i -th row of Y_n .

Let \hat{X} denote an embedding algorithm, or more precisely a sequence of embedding algorithm, one for each dimension n . In the n -th problem the algorithm is given the input Δ_n . We abuse notation by using the symbol \hat{X} to denote embedding regardless of data dimensions n and p_n , so that $\hat{X}(\Delta_n)$ is the result of the embedding algorithm applied to the data Δ_n . Define the asymptotic loss of \hat{X} at \mathbf{x} by

$$L(\hat{X}|\mathbf{x}) \equiv \lim_{n \rightarrow \infty} L_n(\hat{X}(\Delta_n)|X_n)$$

assuming this limit exists. Following Lemma 8 and Lemma 10, it is easy that $L(\hat{X}|\mathbf{x})$ is well defined when \hat{X} is a shrinkage estimator as defined next.

In this asymptotic setting, the decision-theoretical problem becomes simple and well-posed: Nature chooses the value d and the vector $\mathbf{x} \in \mathbb{R}^d$, both unknown to the scientist. The scientist chooses the embedding algorithm \hat{X} , which includes a choice of the embedding dimension r . After both ‘‘players’’ move, the ‘‘payoff’’ is the asymptotic loss $L(\hat{X}|\mathbf{x})$.

2.6. Shrinkage

With the loss function, measuring embedding accuracy, at hand, the questions mentioned in the introduction become more concrete: How does one design an embedding algorithm \hat{X} with

appealing loss for a wide range of possible \mathbf{x} ? Is there an optimal choice of \hat{X} in some sense? As we will see, under the asymptotic loss L , both these questions admit simple, appealing answers.

Truncation estimators. While the classical MDS estimator requires an estimate of the embedding dimension r , we are interested in algorithms that do not require a-priori knowledge or estimation of the embedding dimension. Let us define a “padded” version of the classical MDS algorithm from (13) by

$$\hat{X}^r = \sum_{i=1}^r y_i q_i \mathbf{u}_i \mathbf{e}_i^\top \quad (20)$$

with $e_i \in \mathbb{R}^p$ and $q_1, \dots, q_r \in \{\pm 1\}$. Clearly, \hat{X}^r is just a zero-padded version of \hat{X}^{MDS} , in the sense that

$$\hat{X}^r(\Delta) = \left[\hat{X}^{MDS}(\Delta), \mathbf{0}_{n \times (p-r)} \right].$$

The estimator \hat{X}^r acts by *truncating* the data eigenvalues y_i , keeping only the r largest ones; let us call it the Truncated SVD (TSVD) estimator. As our loss function is invariant under zero padding of the data matrix, it is harmless to use \hat{X}^r instead of \hat{X}^{MDS} . Below, we take the TSVD estimator \hat{X}^r to represent the classical MDS.

In the introduction we mentioned the inherent conundrum involved in choosing the embedding dimension r for classical MDS. Suppose that there exists a function r^* mapping a pair (σ, Δ) , where σ is the noise level and Δ is the observed distance matrix, to an “optimal” choice of embedding dimension r for classical MDS. Formally,

Definition 3 (Optimal TSVD Estimator). *Let $\sigma > 0$. Assume that there exists $\hat{r}^* : \mathbb{R}_+ \times M_{n \times p} \rightarrow \mathbb{N}$ such that*

$$L(\hat{X}^{\hat{r}^*} | \mathbf{x}) \leq L(\hat{X}^r | \mathbf{x})$$

for any $r \in \mathbb{N}$, $d \in \mathbb{N}$ and $x \in \mathbb{R}^d$. Then \hat{r}^ is called the optimal truncation value, and $\hat{X}^{\hat{r}^*}$ is called the optimal TSVD estimator.*

We abuse notation by using \hat{r}^* instead of $\hat{r}^*(\sigma, \Delta)$. Clearly, if such a function \hat{r}^* exists, it would provide a definitive, disciplined manner of choosing the embedding dimension r for classical MDS. As we will see in the next section, \hat{r}^* does indeed exist and admits a simple closed form.

Hard thresholding estimators. The classical MDS estimator, in the form \hat{X}^r , is equivalent to a different estimator, one which uses *hard thresholding* of the data singular values. For $\lambda > 0$, define

$$\hat{X}^\lambda = \sum_{i=1}^n y_i q_i \cdot 1_{[y_i > \lambda]} \mathbf{u}_i \mathbf{e}_i^\top, \quad (21)$$

where $e_i \in \mathbb{R}^p$ and $q_1, \dots, q_n \in \{\pm 1\}$. While \hat{X}^r keeps the r largest data singular values, regardless of their size, the estimator \hat{X}^λ keeps all the data singular values above the hard threshold λ . We call \hat{X}^λ a Singular Value Hard Threshold estimator, or *SVHT*.

It is easy to check that the family of estimators $\{\hat{X}^r\}$ (with data-dependent r) is in fact equivalent to family of estimators $\{\hat{X}^\lambda\}$ (with value of λ fixed a-prior). Formally,

Lemma 5. Let $Y \in M_{n \times p}$ be an observed data matrix, and $\Delta \in M_{n \times n}$ be its corresponding euclidean distance matrix. For any TSVD estimator \hat{X}^r , there exists a SVHT estimator \hat{X}^λ s.t.

$$\hat{X}^r(\Delta) = \hat{X}^\lambda(\Delta)$$

and vice versa.

How should one choose the hard threshold λ ? Suppose that there exists an “optimal” value $\lambda^* > 0$ for which the asymptotic loss is always minimized. Formally,

Definition 4 (Optimal SVHT Estimator). Let $\sigma > 0$. Assume that there is a value $\lambda^* \in [0, \infty)$, which depends on σ and the asymptotic aspect ration β , such that

$$L(\hat{X}^{\lambda^*} | \mathbf{x}) \leq L(\hat{X}^\lambda | \mathbf{x})$$

for any $\lambda > 0$, $d \in \mathbb{N}$ and $\mathbf{x} \in \mathbb{R}^d$. Then λ^* is called an optimal hard threshold, and \hat{X}^{λ^*} is called the optimal SVHT.

For notational simplicity, write λ^* instead of $\lambda_{\beta, \sigma}^*$. As we will see in the next section, λ^* does indeed exist and admits a simple closed form.

The definitions imply that if an optimal hard threshold exists, then it gives rise to an optimal truncation value \hat{r}^* . Formally, it is easy to verify the following.

Definition 5 (SVHT Optimal Cutoff Function). Let $\sigma > 0$. If an optimal hard threshold λ^* exists, then

$$\hat{r}(\Delta) = \#\{i \in [n] \mid y_i > \lambda^*\}$$

is an optimal truncation value.

General shrinkage estimators. The SVHT estimators (21) is a special case of a more general family, which we might call singular value shrinkage estimators. For a non-decreasing function $\eta : [0, \infty) \rightarrow [0, \infty)$, define

$$\hat{X}^\eta = \sum_{i=1}^n \eta(y_i) q_i \mathbf{u}_i \mathbf{e}_i^\top \quad (22)$$

where again $e_i \in \mathbb{R}^p$ and $q_1, \dots, q_n \in \{\pm 1\}$. Observe that \hat{X}^λ is obtained by taking η to be the hard threshold nonlinearity, $\eta(y) = y \cdot \mathbf{1}_{y > \lambda}$.

How should one choose the shrinker η ? Suppose that there exists a special “optimal” shrinker η^* for which the asymptotic loss is always minimized, regardless of the underlying signal. Formally,

Definition 6 (Optimal Continuous Estimator). Let $\sigma > 0$ and let Con denote the family of continuous shrinkers $\eta : [0, \infty) \rightarrow [0, \infty)$. If there exists a shrinker $\eta^* \in Con$ for which

$$L(\hat{X}^{\eta^*} | \mathbf{x}) \leq L(\hat{X}^\eta | \mathbf{x})$$

for any $\eta \in Con$, $d \in \mathbb{N}$ and $x \in \mathbb{R}^d$ then we call η^* an optimal shrinker.

Here too we abuse notation by writing η^* for $\eta_{\beta, \sigma}^*(\Delta)$. As we show in the next section, the optimal shrinker η^* does exist and admits a simple form.

3. Results

For simplicity, we state our results first for the case where the noise level σ is known. The case of σ unknown is deferred to the end of the section.

As seen in lemma 2, classical MDS achieves zero loss, or perfect reconstruction of the original data, in the noiseless case $\sigma = 0$. Our first main result is the exact asymptotic loss incurred by classical MDS in the presence of noise.

Theorem 1. *The asymptotic loss of classical MDS with embedding dimension r is given by*

$$L(\hat{X}^r | \mathbf{x}) \stackrel{a.s.}{=} \left(\sum_{i=1}^{\min(t,r)} \left(\sqrt{x_i^2 + \sigma^2} - \sqrt{\frac{x_i^4 - \beta \cdot \sigma^4}{x_i^2}} \right)^2 + \frac{2 \cdot \beta \cdot \sigma^4}{x_i^2} + \beta \cdot \sigma^2 \right) + \left(\sum_{j=\min(t,r)+1}^d x_j^2 \right) + (r-t)^+ \cdot \sigma^2 \cdot (1 + \sqrt{\beta})^2 \quad (23)$$

where $t = \#\{i \in [d] \text{ s.t. } x_i > \sigma \cdot \beta^{\frac{1}{4}}\}$.

As discussed in subsection 2.6 above, for a specific dataset, classical MDS is equivalent to singular value hard thresholding (SVHT) at a hard threshold that depends on the data. An obvious way to improve the classical MDS algorithm is to consider a carefully calibrated choice of hard threshold. Our next result shows that, in fact, an asymptotically optimal choice of hard threshold exists – and even admits a simple closed form.

Theorem 2. *There exists a unique optimal hard threshold λ^* (Definition 4), and its value is given by*

$$\lambda = \sigma \cdot \sqrt{\left(\sqrt{a} + \frac{1}{\sqrt{a}} \right) \left(\sqrt{a} + \frac{\beta}{\sqrt{a}} \right)} \quad (24)$$

where a is the unique positive root of

$$-3 \cdot a^3 + a^2 \cdot (2\beta + 1) + a \cdot (\beta^2 + 6 \cdot \beta) + \beta^2 = 0.$$

Moreover, $\lambda^* > \sigma \cdot (1 + \sqrt{\beta})$.

It now follows from Lemma 5 that we have obtained an optimal choice of embedding dimension for classical MDS:

Corollary 1. *The quantity*

$$\hat{r}^* = \#\{i \in [n] : y(x_i) > \lambda^*\} \quad (25)$$

is an optimal truncation value (Definition 3).

So far we have shown that an optimal truncation value \hat{r}^* and the optimal hard threshold λ^* exist. In fact, an optimal shrinker also exists:

Theorem 3. *There exists a unique optimal shrinker η^* (Definition 6) given by*

$$\eta^*(y) \stackrel{a.s.}{=} \begin{cases} \sigma \sqrt{(x(y)/\sigma)^2 - \beta - \frac{\beta \cdot (1-\beta)}{(x(y)/\sigma)^2 + \beta}} & y > \sigma \cdot (1 + \sqrt{\beta}) \\ 0 & \text{otherwise} \end{cases} \quad (26)$$

where

$$x(y) = \frac{\sigma}{\sqrt{2}} \sqrt{\left(\frac{y}{\sigma}\right)^2 - 1 - \beta + \sqrt{\left(\left(\frac{y}{\sigma}\right)^2 - 1 - \beta\right)^2 - 4\beta}}. \quad (27)$$

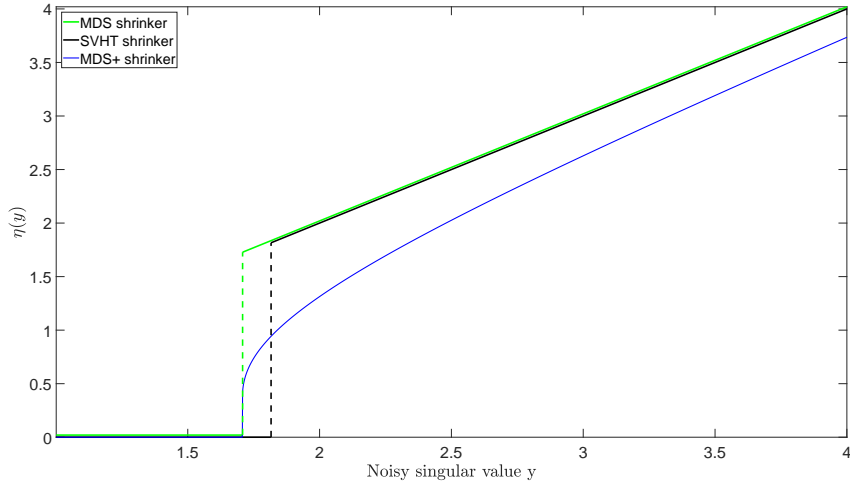


Figure 7: The shrinkers function over the singular value of a rank-1 original matrix X . Here, $\beta = 0.5$ and $\sigma = 1$. (Color online)

The estimator \hat{X}^{η^*} , with the optimal shrinker η^* is a simple alternative to classical MDS, which we call MDS+. (The algorithm is written explicitly in table 2, located in subsection 1.3)

We next consider the asymptotic loss obtained by the optimal shrinker η^* .

Theorem 4. *The asymptotic loss of the optimal shrinker η^* is:*

$$L(\hat{X}^{\eta^*} | \mathbf{x}) \stackrel{a.s.}{=} \beta \cdot \sigma^2 \cdot \left(\sum_{i=1}^t \frac{1-\beta}{(x_i/\sigma)^2 + \beta} + 1 \right) + \sum_{i=t+1}^d x_i^2 \quad (28)$$

where $t = \#\{i \in [d] \text{ s.t. } x_i > \sigma \cdot \beta^{\frac{1}{4}}\}$.

Our next main result quantifies the regret for using the classical MDS (even with optimally tuned with the optimal truncation value \hat{r}^*) instead of the the proposed algorithm MDS+.

Theorem 5. Let $r \in \mathbb{N}$ and consider the classical MDS with embedding dimension r . The asymptotic loss of $MDS+$ is a.s. better than the asymptotic loss of classical MDS, and in fact the quantity

$$\begin{aligned}
L(\hat{X}^r|X) - L(\hat{X}^{\eta^*}|X) &\stackrel{a.s.}{=} \left(\sum_{i=1}^t \mathbf{1}_{[i \leq r]} \left[\left(\sqrt{x_i^2 + \sigma^2} - \sqrt{\frac{x_i^4 - \beta \cdot \sigma^4}{x_i^2}} \right)^2 \right. \right. \\
&\quad \left. \left. + \beta \cdot \sigma^2 \cdot \frac{(x_i/\sigma)^2 \cdot (1 + \beta) + 2\beta}{(x_i/\sigma)^4 + \beta \cdot (x_i/\sigma)^2} \right] \right. \\
&\quad \left. + \mathbf{1}_{[i > r]} \cdot \sigma^2 \cdot \frac{(x_i/\sigma)^4 - \beta}{(x_i/\sigma)^2 + \beta} \right) \\
&\quad + \sum_{i=t+1}^r \sigma^2 \cdot (1 + \sqrt{\beta})^2 \\
&\geq 0,
\end{aligned}$$

is always non-negative. Here, $t = \#\{i \in [d] \text{ s.t. } x_i > \sigma \cdot \beta^{\frac{1}{4}}\}$.

Figure 8 shows the regret over the signal singular value x for specific values of r, β and σ .

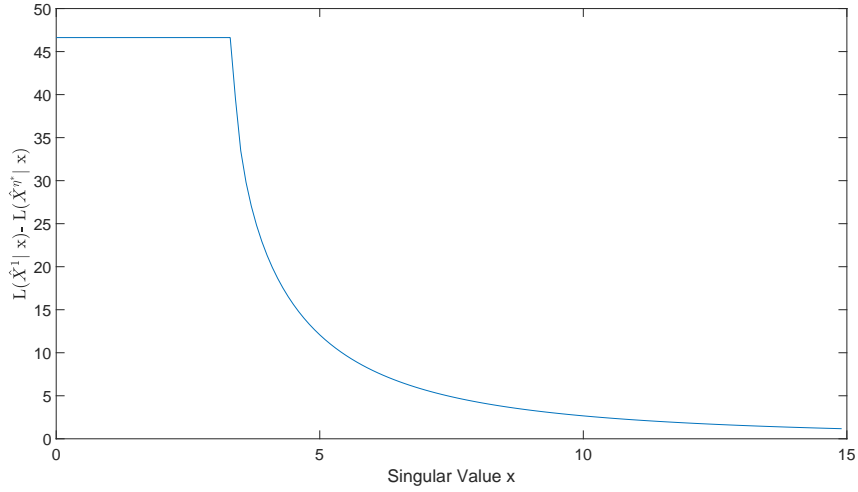


Figure 8: Regret, in terms of asymptotic loss, for using MDS (with embedding dimension set at 1) instead of $MDS+$. Here, $r = 1$, $\sigma = 4$ and $\beta = 0.5$

Estimating the noise level σ . When the noise level σ is unknown, it must be estimated in order to use $MDS+$. A number of approaches were developed over the years for estimating the noise level [32, 36, 37]. Here we follow the proposal of [33], which showed:

Theorem 6. Consider

$$\hat{\sigma}(S) = \sqrt{\frac{S_{med}}{19 \mu_{\beta}}} \quad (29)$$

where $s_1 \geq \dots \geq s_{\min(n,p)} \geq 0$ are the eigenvalues of S , and s_{med} is their median. Denote the median of the Marcenko Pastur (MP) distribution [38] for β by μ_β . Then $\hat{\sigma}^2(S_n) \xrightarrow{a.s.} \sigma^2$ as $n \rightarrow \infty$.

The MP median is not available analytically yet is very simple to calculate numerically (see the Code Supplement [16]). It is easy to verify that by plugging in $\hat{\sigma}$ for σ , the main results above hold.

Figure 9 compares the asymptotic loss of classical MDS, optimally tuned SVHT, and MDS+.

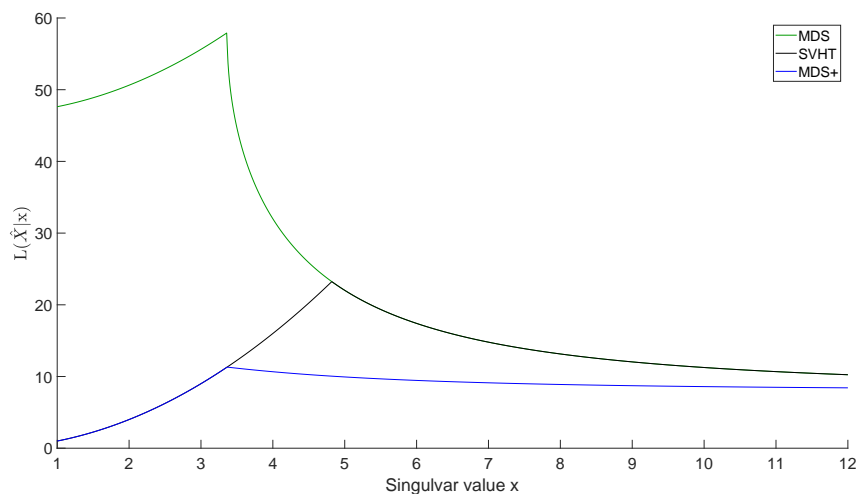


Figure 9: The asymptotic loss of classical MDS (with embedding dimension set to 1), optimally tuned SVHT and MDS+. Here $\sigma = 4$, $p = 500$ and $n = 251$. (Color online)

The case $\beta > 1$. So far, we only considered the case $\beta \in (0, 1]$. The Appendix contains similar results for the case $\beta \geq 1$.

4. Discussion

Implications on Manifold Learning. Manifold learning and metric learning methods seek to reconstruct a global, low-dimensional geometric structure of a dataset from pairwise dissimilarity or affinity measurements [1, 2, 3, 4, 5, 6, 7]. As such, they are specifically designed to be applied to data in high-dimensional Euclidean spaces. However, the manifold learning literature contains very little reference to the sensitivity of these methods to measurement noise, and particularly to ambient noise contaminating the data observed in high-dimensional space.

The results of the present paper show conclusively that the effect of measurement noise cannot be ignored. Indeed, we have shown that the behavior of MDS, arguably the earliest and one of the most widely-used Euclidean embedding techniques, and a linear precursor to manifold learning techniques, depends crucially on the measurement noise level σ . For instance, Theorem 1 shows that classical MDS breaks down whenever any one of the singular values x of the signal falls below the critical point $\sigma \cdot \beta^{1/4}$.

These phenomena necessarily hold in any manifold learning technique which relies on spectral decomposition of similarity distances, which is to say, in basically any manifold learning technique. In this regard our results call for a thorough investigation of the noise sensitivity of many well known manifold learning methods in the presence of noisy, high dimensional measurements. We expect that the phenomena formally quantified in this paper, including breakdown of the method in a critical noise level, are all present in basically any manifold learning method.

Formal quantification of embedding quality. Dimensionality reduction and manifold learning techniques are non-supervised. As such, the literature has traditionally ignored their formal operating characteristics and focused on asymptotic theorems showing that certain manifold quantities are recovered, as well as examples where they appear to perform well, relying on visualizations to demonstrate how a method of interest can be expected to perform. The present paper takes a decision-theoretical approach, and evaluates the performance of a non-supervised learning method (in this case, MDS) using a loss function. We place our choice of loss function on solid footing with a combination of three results:

1. In the absence of noise, the classical MDS algorithm is recovered by minimizing the proposed loss (Lemma 2).
2. The proposed loss function satisfies invariance properties which any reasonable loss function should satisfy (Lemma 3).
3. The loss function is based on a pseudo-metric (Lemma 4).

By introducing a loss function, analysis and comparison of different methods become possible and even simple. It also gives rise to the notion of an optimal method.

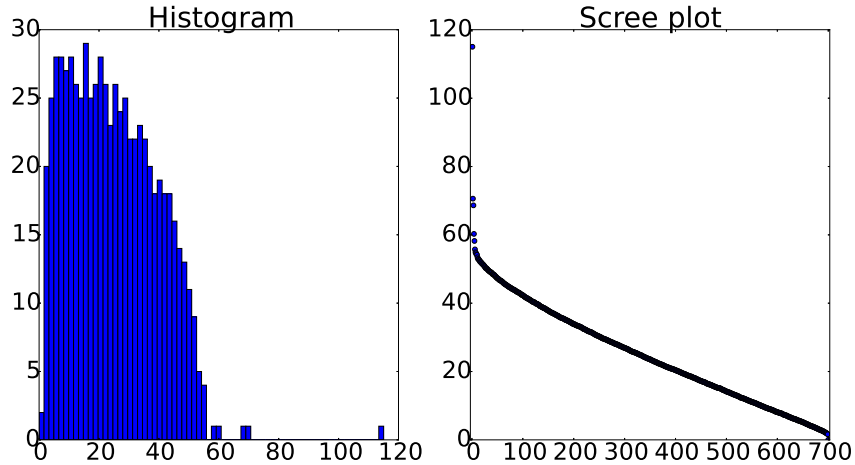


Figure 10: Histogram of singular values (left) and Scree plot of singular values (right) of MNIST data, see Figure 3 above. Here the noise level we used is $\sigma = 30$, implying noise standard deviation $\sigma/\sqrt{p} = 30/\sqrt{784} \approx 1.07$.

Bulk edge, Scree plot and the optimal threshold λ^ .* It is interesting to compare quantitatively the SVHT method with optimal threshold λ^* from Theorem 2 with the classical Scree plot method. While the Scree plot method itself is not a formally specified algorithm (it is actually more of a subjective a visual ceremony) we argue that it is roughly equivalent to hard thresholding of the singular values (as in (13) and (20)), with a specific choice of threshold. Plotting a histogram of the singular values (Figure 10, left panel) instead of their Scree plot (right panel) one observes that the so-called “bulk” of singular values in lower part of the histogram is the density of noise-only singular values, known as the Quarter Circle distribution [39], with compactly supported density

$$f_{QC}(x) = \begin{cases} \frac{\sqrt{4\beta\sigma^4 - (x^2 - \sigma^2 - \beta\sigma^2)^2}}{\pi\sigma^2\beta \cdot x} & \text{if } x \in [\lambda_-, \lambda_+] \\ 0 & \text{otherwise} \end{cases} \quad (30)$$

where $\lambda_{\pm} = \sigma \cdot (1 \pm \sqrt{\beta})$ and $\beta \in (0, 1]$. The upper edge of the support, known as the “bulk edge” is located at λ_+ . Comparing histograms of various noise distributions with their respective Scree plots, one easily observes that the famous “knee” or “elbow” in Cattell’s Scree plot [15] is simply the location of the bulk edge. It follows that the Scree plot ceremony is roughly equivalent to an attempt to visually locate the bulk edge of the underlying noise-only distribution.

It is interesting to observe that the optimal threshold λ^* is always larger than the bulk edge. In other words, even when the singular values are visually recognizable above the elbow in the Scree plot, and are detectable as signal singular values (distinct from the noise singular values) it is still worthwhile, from the perspective of the asymptotic loss, to exclude them from the reconstruction, as long as they are “too close” to the bulk edge. For a more thorough discussion of this phenomena, see [33].

Figure 11 compares the asymptotic loss of the classical MDS (with the Scree plot ceremony, namely bulk-edge hard thresholding), MDS with the optimal threshold λ^* and MDS+ – equations (13), (24) and (26) respectively, over the signal singular value x .

Accuracy in finite- n . The threshold and shrinker derived in this paper are based on an asymptotic loss, and one naturally wonders whether they remain approximately optimal in finite values of n . While this question is beyond our present scope, we note that the convergence to the limit of the loss and its underlying components is rapid and indeed the asymptotically optimal threshold and shrinker can be used in practice. Figure 11 shows the predicted asymptotic loss (solid lines) and the empirically observed mean and standard deviation from a Monte-Carlo simulation. Precise evaluation of the finite- n effects will be evaluated elsewhere.

5. Proofs

5.1. Notation

Following subsection 2.5, we assume the same d singular values over all X_n . Denote its singular values by $\mathbf{x} = (x_1, \dots, x_d)$, as assumed they are non-degenerate, so that $x_1 > \dots > x_d > 0$, and they are mean centered, so that $H \cdot X_n = X_n$. Denote its left and right singular vectors as $\{\mathbf{v}_{n,1}, \dots, \mathbf{v}_{n,n}\} \subset \mathbb{R}^n$ and $\{\tilde{\mathbf{v}}_{n,1}, \dots, \tilde{\mathbf{v}}_{n,d}\} \subset \mathbb{R}^d$, respectively. Denote the corresponding matrices of singular vectors by $V_n = [\mathbf{v}_{n,1}, \dots, \mathbf{v}_{n,n}] \in O(n)$ and $\tilde{V}_n = [\tilde{\mathbf{v}}_{n,1}, \dots, \tilde{\mathbf{v}}_{n,d}] \in O(d)$. Similarly, denote the singular values of $H \cdot Y_n$ by $y_{n,1} \geq \dots \geq y_{n,p_n} \geq 0$ and its left and right singular vectors by $\{\mathbf{u}_{n,1}, \dots, \mathbf{u}_{n,n}\} \in \mathbb{R}^d$ and $\{\tilde{\mathbf{u}}_{n,1}, \dots, \tilde{\mathbf{u}}_{n,n}\} \in \mathbb{R}^{p_n}$, respectively. Let the corresponding singular vector matrices be $U_n = [\mathbf{u}_{n,1}, \dots, \mathbf{u}_{n,n}] \in O(n)$ and $\tilde{U}_n = [\tilde{\mathbf{u}}_{n,1}, \dots, \tilde{\mathbf{u}}_{n,p_n}] \in O(p_n)$.

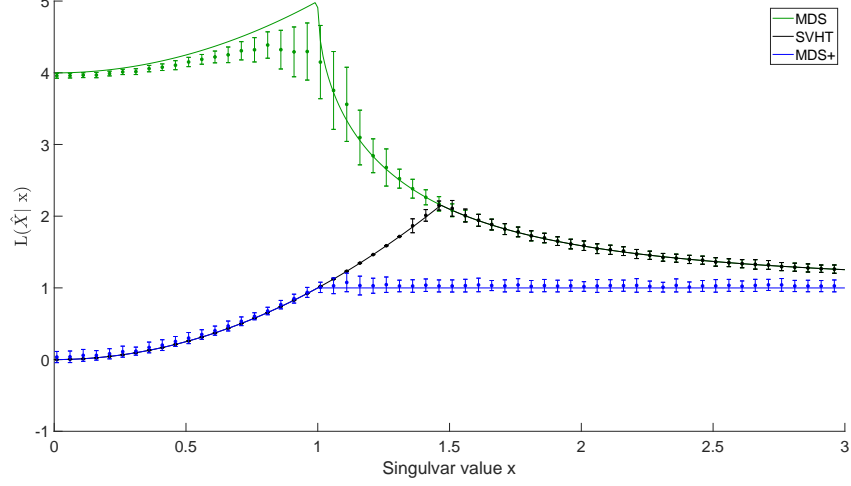


Figure 11: $X \in M_{1000 \times 1000}$, $d = 1$, $r = 1$, $\sigma = 1$. The plot is composed of 100 tests for each singular value. The points indicates the mean of the loss over the tests, while the error bars indicate the standard deviation of the tests. The solid line indicates the theoretic loss (Color online)

Some properties of the centering matrix H are important in what follows. Denote $H = U_H \cdot D_H \cdot U_H^\top$ as its eigenvalue Decomposition, where $U_H \in O(n)$ is the eigenvector matrix and $D_H = \text{diag}(1, \dots, 1, 0)$ is the eigenvalue matrix. Observe that $(U_H)_{*,n} = \frac{1}{\sqrt{n}} \mathbf{1}_n$ and that $H \cdot H = H$ as the centering matrix is a projection. While H depends on n , we suppress it and leave it to be inferred from context.

5.2. Limiting location of the singular values and vectors

Lemma 6. *The asymptotic distribution of $H \cdot Y$ has the following properties for any finite i and j :*

1. $\lim_{n \rightarrow \infty} y_{n,i} \stackrel{a.s.}{=} \begin{cases} y(x_i) & i \in [t] \\ \sigma \cdot (1 + \sqrt{\beta}) & \text{otherwise} \end{cases}$
2. $\lim_{n \rightarrow \infty} |\langle \mathbf{u}_{n,i}, \mathbf{v}_{n,j} \rangle| \stackrel{a.s.}{=} \begin{cases} c(x) & i = j \in [t] \\ 0 & \text{otherwise} \end{cases}$

when $t \equiv \#\{i \in [d] \mid |x_i/\sigma| > \beta^{\frac{1}{4}}\}$ and

$$c(x) = \sqrt{\frac{(x/\sigma)^4 - \beta}{(x/\sigma)^4 + \beta(x/\sigma)^2}}$$

$$y(x) = \sqrt{\left(x/\sigma + \frac{1}{x/\sigma}\right) \cdot \left(x/\sigma + \frac{\beta}{x/\sigma}\right)}$$

In order to prove Lemma 6 we'll need the following result:

Lemma 7. *We have*

$$H \cdot Y = U_H \cdot \begin{bmatrix} \sum_{i=1}^d x_i \cdot (I_{n-1 \times n} \cdot U_H^\top \cdot \mathbf{v}_i) \cdot [\tilde{\mathbf{v}}_i^\top, \mathbf{0}_{\mathbf{p}-d}^\top] + \frac{1}{p} \dot{Z}_{1:n-1,*} \\ \mathbf{0}_d^\top \end{bmatrix} \cdot R \quad (31)$$

Where $\dot{Z} \sim Z$, and $U_H \in O(n)$ is the eigenvectors matrix form of the Eigenvalue Decomposition of H .

Proof. Another way of writing $H \cdot Y$ is:

$$H \cdot Y = H \cdot (Y \cdot I_{d \times p} \cdot R + \frac{1}{p} Z) = U_H \cdot D_H \cdot U_H^\top \cdot (H \cdot Y \cdot I_{d \times p} + \frac{1}{p} \dot{Z}) \cdot R \quad (32)$$

where $\dot{Z} \equiv Z \cdot R^\top$. (31) follows since

$$\begin{aligned} D_H \cdot U_H^\top \cdot (H \cdot Y \cdot I_{d \times p} + \frac{1}{p} \dot{Z}) &= D_H \cdot (\sum_{i=1}^d x_i \cdot (U_H^\top \cdot \mathbf{v}_i) \cdot [\tilde{\mathbf{v}}_i^\top, \mathbf{0}_{\mathbf{p}-d}^\top] + \frac{1}{p} \dot{Z}) \\ &= \begin{bmatrix} \sum_{i=1}^d x_i \cdot (I_{n-1 \times n} \cdot U_H^\top \cdot \mathbf{v}_i) \cdot [\tilde{\mathbf{v}}_i^\top, \mathbf{0}_{\mathbf{p}-d}^\top] + \frac{1}{p} \dot{Z}_{1:n-1,*} \\ \mathbf{0}_p^\top \end{bmatrix} \end{aligned}$$

where $\dot{Z} \equiv U_H \cdot \dot{Z}$. $\dot{Z} \sim Z$ follows from the invariant white noise property of the framework, as defined in subsection 2.5. \square

Proof of Lemma 6. Following lemma 7

$$U_H^\top \cdot H \cdot Y_n \cdot R_n^\top = \begin{bmatrix} \sum_{i=1}^d x_i \cdot (I_{n-1 \times n} \cdot U_H^\top \cdot \mathbf{v}_{n,i}) \cdot [\tilde{\mathbf{v}}_{n,i}^\top, \mathbf{0}_{\mathbf{p}_n-d}^\top] + \frac{1}{p_n} (\dot{Z}_n)_{1:n-1,*} \\ \mathbf{0}_{\mathbf{p}_n}^\top \end{bmatrix}$$

First we define $W_n \equiv \sum_{i=1}^d x_i \cdot (I_{n-1 \times n} \cdot U_H^\top \cdot \mathbf{v}_{n,i}) \cdot [\tilde{\mathbf{v}}_{n,i}^\top, \mathbf{0}_{\mathbf{p}_n-d}^\top] \in M_{n-1 \times p_n}$ and show that this is an acceptable SVD decomposition of W_n .

We start by showing that $\{I_{n-1 \times n} \cdot U_H^\top \cdot \mathbf{v}_{n,i}\}_{i=1}^d$ is an orthonormal set, where $d = \text{rank}(X_n)$. Now, we can see that $(U_H)_{*,n} = \frac{1}{\sqrt{n}} \mathbf{1}_n \in \text{span} \{ \{\mathbf{v}_{n,k}\}_{k=d+1}^n \}$ following the assumption that $X_n = H \cdot X_n$, and $\text{rank}(X_n) = d$. Therefore for any $i \in \{1, \dots, d\}$

$$\langle \mathbf{e}_n, U_H^\top \cdot \mathbf{v}_{n,i} \rangle = \langle \frac{1}{\sqrt{n}} \mathbf{1}_n, \mathbf{v}_{n,i} \rangle = 0 \quad (33)$$

since $\{\mathbf{v}_{n,i}\}$ is an orthogonal set. Therefore for any $i, j \in \{1, \dots, d\}$:

$$\begin{aligned} \langle I_{n-1 \times n} \cdot U_H^\top \cdot \mathbf{v}_{n,i}, I_{n-1 \times n} \cdot U_H^\top \cdot \mathbf{v}_{n,j} \rangle &= \\ \langle U_H^\top \cdot \mathbf{v}_{i,n}, (I_n - \mathbf{e}_n \cdot \mathbf{e}_n^\top) \cdot U_H^\top \cdot \mathbf{v}_{n,j} \rangle &= \\ \langle U_H^\top \cdot \mathbf{v}_{n,i}, U_H^\top \cdot \mathbf{v}_{n,j} \rangle - 0 = \langle \mathbf{v}_{n,i}, \mathbf{v}_{n,j} \rangle &= \mathbf{1}_{[i=j]} \end{aligned}$$

The set $\left\{ \begin{pmatrix} \tilde{\mathbf{v}}_{n,i} \\ \mathbf{0}_{\mathbf{p}_n-d} \end{pmatrix} \right\}_{i=1}^d$ is an orthonormal set also simply because $\{\tilde{\mathbf{v}}_{n,i}\}_{i=1}^d$ is an orthonormal set.

Second, we define $Q_n \equiv W_n + \frac{1}{p_n}(\hat{Z}_n)_{1:n-1,*}$ and denote its SVD decomposition form by

$$Q_n = \sum_{i=1}^{n-1} q_{n,i} \cdot \mathbf{w}_{n,i} \tilde{\mathbf{w}}_{n,i}^\top$$

where $\mathbf{w}_{n,i} \in \mathbb{R}^{n-1}$ and $\tilde{\mathbf{w}}_{n,i} \in \mathbb{R}^{p_n}$ are its i -th left and right singular vectors, respectively, and $q_{n,i}$ is its i -th singular value. We would like to emphasize the relations between Q_n and W_n at the limit.

Denote the singular values of $(\hat{Z}_n/p_n)_{1:n-1,*}$ by $z_1 \geq \dots \geq z_{n-1}$. Following [39] the density of the singular values of \hat{Z}_n/p_n in the limit is the quarter-circle density:

$$f(x) = \frac{\sqrt{4\beta\sigma^4 - (x^2 - \sigma^2 - \beta\sigma^2)^2}}{\pi\beta\sigma^2 \cdot x},$$

following [40] $y_{n,1} \xrightarrow{a.s.} \sigma \cdot (1 + \sqrt{\beta})$, and following [41] $y_{n,\min(n,p_n)} \xrightarrow{a.s.} \sigma \cdot (1 - \sqrt{\beta})$. These satisfies assumptions 2.1,2.2 and 2.3 in [31], respectively, therefore for any finite i :

1. Translation of singular values:

$$\lim_{n \rightarrow \infty} q_{n,i} \stackrel{a.s.}{=} \begin{cases} y(x_i) & \text{if } x_i/\sigma > \beta^{1/4} \\ \sigma \cdot (1 + \sqrt{\beta}) & \text{otherwise} \end{cases}$$

2. Rotation of the left singular vectors:

$$\lim_{n \rightarrow \infty} |\langle U_H^\top \cdot \mathbf{v}_{n,i}, \mathbf{w}_{n,j} \rangle| \stackrel{a.s.}{=} \begin{cases} c(x_i) & \text{if } x_i/\sigma > \beta^{1/4} \text{ and } i = j \\ 0 & \text{otherwise} \end{cases}$$

where

$$c(x) = \sqrt{\frac{(x/\sigma)^4 - \beta}{(x/\sigma)^4 + \beta(x/\sigma)^2}}$$

$$y(x) = \sqrt{(x/\sigma + \frac{1}{x/\sigma}) \cdot (x/\sigma + \frac{\beta}{x/\sigma})}$$

Third we denote $W_n^L \equiv \begin{bmatrix} W_n \\ \mathbf{0}_{p_n}^\top \end{bmatrix}$ and $Q_n^L \equiv \begin{bmatrix} Q_n \\ \mathbf{0}_{p_n}^\top \end{bmatrix}$. Following equation (33), those matrices could be expressed in a singular value decomposition form using W_n and Q_n , respectively, by

$$W_n^L = \sum_{i=1}^d x_i \cdot \begin{bmatrix} (I_{n-1 \times n} \cdot U_H^\top \cdot \mathbf{v}_{n,i}) \\ 0 \end{bmatrix} \cdot [\tilde{\mathbf{v}}_{n,i}^\top, \mathbf{0}_{p_n-d}^\top]$$

$$= \sum_{i=1}^d x_i \cdot (U_H^\top \cdot \mathbf{v}_{n,i}) \cdot [\tilde{\mathbf{v}}_{n,i}^\top, \mathbf{0}_{p_n-d}^\top]$$

$$Q_n^L = \sum_{i=1}^{n-1} q_{n,i} \cdot \begin{bmatrix} \mathbf{w}_{n,i} \\ 0 \end{bmatrix} \tilde{\mathbf{w}}_{n,i}^\top$$

Another valid way of writing Q_n^L in a singular value decomposition components form is

$$Q_n^L = U_H^T \cdot H \cdot Y \cdot R_n^T = \sum_{i=1}^n y_i \cdot (U_H^T \cdot \mathbf{u}_{n,i}) \cdot (\tilde{\mathbf{u}}_{n,i}^T \cdot R_n^T)$$

since R_n, U_H are orthogonal matrices. Therefore for any finite i holds

1. Translation of singular values:

$$\lim_{n \rightarrow \infty} y_{n,i} \stackrel{a.s.}{=} \begin{cases} y(x_i) & \text{if } x_i/\sigma > \beta^{1/4} \\ \sigma \cdot (1 + \sqrt{\beta}) & \text{otherwise} \end{cases}$$

following the fact that for any n and any i $q_{n,i} = y_{n,i}$.

2. Rotation of the left singular vectors:

$$\lim_{n \rightarrow \infty} |\langle \mathbf{v}_{n,i}, \mathbf{u}_{n,j} \rangle| = \lim_{n \rightarrow \infty} \left| \left\langle U_H^T \cdot \mathbf{v}_{n,i}, \begin{bmatrix} \mathbf{w}_{n,j} \\ 0 \end{bmatrix} \right\rangle \right| \stackrel{a.s.}{=} \begin{cases} c(x_i) & \text{if } x_i > \sigma \cdot \beta^{1/4} \text{ and } i = j \\ 0 & \text{otherwise} \end{cases}$$

since $\langle \mathbf{v}_{n,i}, \mathbf{u}_{n,j} \rangle = \langle U_H^T \cdot \mathbf{v}_{n,i}, U_H^T \cdot \mathbf{u}_{n,j} \rangle$ for any n .

□

5.3. MDS loss function analysis

In the following subsection the index n is suppressed to simplify notation.

Theorem 7. Let $\Delta \in \mathbb{R}^{n \times n}$ be an Euclidean distance matrix over the dataset $\{b_i\}_{i=1}^n$, namely, $\Delta_{i,j} = \|b_i - b_j\|_2^2$. The similarity matrix (2), used in the classical MDS algorithm, satisfies

$$S = H \cdot Y \cdot (H \cdot Y)^T. \quad (34)$$

Moreover, $S_{i,j} = \langle \mathbf{b}_i - \mu_{\mathbf{b}}, \mathbf{b}_j - \mu_{\mathbf{b}} \rangle$, where $\mu_{\mathbf{b}} = \frac{1}{n} \sum_{i=1}^n \mathbf{b}_i$ is the empirical mean.

Proof. Another way of writing the distance matrix is:

$$\Delta = \text{diag}(Y \cdot Y^T) \cdot \mathbf{1}_n^T + \mathbf{1}_n \cdot \text{diag}(Y \cdot Y^T) - 2 \cdot Y \cdot Y^T.$$

Indeed, this follows from $\Delta_{i,j} = \|\mathbf{b}_i\|_2^2 + \|\mathbf{b}_j\|_2^2 - 2\langle \mathbf{b}_i, \mathbf{b}_j \rangle$. Equation (34) now follows since

$$\begin{aligned} S &= -\frac{1}{2} \left(I_n - \frac{1}{n} \cdot \mathbf{1} \cdot \mathbf{1}^T \right) \cdot \Delta \cdot \left(I_n - \frac{1}{n} \cdot \mathbf{1} \cdot \mathbf{1}^T \right) \\ &= -\frac{1}{2} \cdot \left(I_n - \frac{1}{n} \cdot \mathbf{1} \cdot \mathbf{1}^T \right) \cdot (-2 \cdot Y \cdot Y^T) \cdot \left(I_n - \frac{1}{n} \cdot \mathbf{1} \cdot \mathbf{1}^T \right) \\ &= H \cdot Y \cdot (H \cdot Y)^T, \end{aligned}$$

where we have used

$$\text{diag}(Y \cdot Y^T) \cdot \mathbf{1}^T \cdot \left(I_n - \frac{1}{n} \cdot \mathbf{1} \cdot \mathbf{1}^T \right) = \text{diag}(Y \cdot Y^T) \cdot \mathbf{1}^T - \text{diag}(Y \cdot Y^T) \cdot \mathbf{1}^T = \mathbf{0}_{n \times n}.$$

Now, each entry of the similarity matrix is simply

$$S_{i,j} = (H \cdot Y)_{i,*} \cdot (H \cdot Y)_{j,*}^\top = \langle \mathbf{b}_i - \mu_{\mathbf{b}}, \mathbf{b}_j - \mu_{\mathbf{b}} \rangle,$$

since

$$(H \cdot Y)_{i,j} = (I - \frac{1}{n} \mathbf{1}_n \mathbf{1}_n^\top)_{i,*} \cdot Y_{*,j} = Y_{i,j} - \frac{1}{n} \sum_{k=1}^n Y_{i,k} = (\mathbf{b}_i)_j - \frac{1}{n} \sum_{k=1}^n (\mathbf{b}_k)_j.$$

□

Theorem 8. Let $\sigma = 0$ and the embedding dimension be $r = d$. The MDS embedding result has the following property:

$$\hat{\mathbf{a}}_i = S \cdot \mathbf{a}_i \quad (35)$$

for some $S \in O(d)$, where $\hat{\mathbf{a}}_i$ is the reconstruction of \mathbf{a}_i .

Proof. The noiseless configuration is

$$Y = [X, 0_{d \times p}] \cdot R$$

It follows that $H \cdot Y = Y$ since we have assumed that $H \cdot X = X$. Following Theorem 7, the similarity matrix could be described using X 's SVD decomposition components:

$$S = (HY) \cdot (HY)^\top = (H \cdot [X, 0_{d \times p}] \cdot R) \cdot (H \cdot [X, 0_{d \times p}] \cdot R)^\top = X \cdot X^\top = \sum_{i=1}^d x_i \cdot \mathbf{v}_i \mathbf{v}_i^\top$$

It follows from (13) that the MDS algorithm (with embedding dimension d) results in

$$\hat{X}^{MDS} = \sum_{i=1}^d x_i q_i \cdot \mathbf{v}_i \mathbf{e}_i^\top \in M_{n \times d}$$

where $q_1, \dots, q_d \in \{\pm 1\}$. Equation (35) now follows while plugging in $S^\top = \tilde{V} \cdot \text{diag}(q_1, \dots, q_d) \in O(d)$ as the orthogonal matrix

$$\hat{X}^{MDS} = X \cdot S^\top$$

or in its vector form

$$\hat{a}_i = S \cdot a_i \quad i=1, \dots, r$$

□

Proof of Theorem 2. As seen in the proof of Theorem 8, $H \cdot Y$ could be written using its SVD decomposition components

$$H \cdot Y = Y = \sum_{i=1}^d x_i \cdot \mathbf{v}_i \cdot \left(R^\top \cdot \begin{pmatrix} \tilde{\mathbf{v}}_i \\ \mathbf{0}_{p-d} \end{pmatrix} \right)^\top$$

By Theorem 7, in this case we have $\text{rank}(S) = \text{rank}(H \cdot Y) = d$. Denote the MDS embedding for any r by \hat{X}_r^{MDS} . It follows from (13) that the result of the MDS embedding is

$$\hat{X}_r^{MDS} = \sum_{i=1}^{\min(r,d)} x_i q_i \cdot \mathbf{v}_i \mathbf{e}_i^\top$$

where $e_i \in \mathbb{R}^r$ and $q_i \in \{\pm 1\}$ for any $i \in \{1, \dots, r\}$. Meaning that for any $r_1, r_2 \geq d$ holds

$$M_n(\hat{X}_{r_1}^{MDS}, X) = M_n(\hat{X}_{r_2}^{MDS}, X) = 0$$

Therefore the MDS's embedding result is in the set of optimal embeddings that minimizes $M_n(\cdot, X)$ since $M_n(\cdot, \cdot) \geq 0$. \square

Proof of Theorem 3. The rotation invariance property is a direct result of the minimizers' domain, which is a group that is closed under multiplication. The translation invariance property is a direct result of the similarity distance definition where the mean of each dataset is taken off the dataset before trying to find the optimal minimizer. This function is invariant for zero-padding as a direct result of the zero padding property of the actual definition, meaning that $M_n(Y_1, Y_2) = M_n([Y_1, 0_{n \times k}], Y_2)$ for any k . Now, the padding invariance is achieved using the zero-padding invariance property and the translation invariance discussed above. Meaning, for any k and any $c \in \mathbb{R}^k$ holds

$$M_n \left(\begin{pmatrix} c^T \\ Y_1, \\ c^T \\ \dots \\ c^T \end{pmatrix}, Y_2 \right) = M_n([Y_1, 0_{n \times k}], Y_2) = M_n(Y_1, Y_2)$$

\square

Proof of lemma 4. The first property holds, by simply using $R = I_d$. The second property can be derived as follows

$$\begin{aligned} M_n(X, Y) &= \min_{R \in O(n)} \|X - Y \cdot R\| \\ &= \min_{R \in O(n)} \|X \cdot R^T - Y\| \\ &= \min_{Q \in O(n)} \|X \cdot Q - Y\| \\ &= M_n(Y, X) \end{aligned}$$

since $O(n)$ is a group that is closed under multiplication and $R^{-1} = R^\top$ for any $R \in O(n)$. For the triangle inequality property we are going to derive a similar property for start

$$\begin{aligned} M_n(X, Y) &= \min_{R \in O(n)} \|X - Y \cdot R\| \\ &= \min_{R \in O(n)} \|X - Z \cdot Q + Z \cdot Q - Y \cdot R\| \\ &\leq \min_{R \in O(n)} \|X - Z \cdot Q\| + \|Z \cdot Q - Y \cdot R\| \\ &= \|X - Z \cdot Q\| + \min_{R \in O(n)} \|Z - Y \cdot R \cdot Q^\top\| \\ &= \|X - Z \cdot Q\| + \min_{W \in O(n)} \|Z - Y \cdot W\| \end{aligned}$$

where $Q \in O(n)$. The triangle inequality property follows since

$$M_n(X, Y) \leq \|X - Z \cdot Q\| + \min_{W \in O(n)} \|Z - Y \cdot W\| = M_n(X, Z) + M_n(Z, Y)$$

where Q is the minimizer of $M_n(X, Z)$. \square

5.4. MDS loss function estimation

Lemma 8. *Let $d \in \mathbb{N}$. For any matrix $X \in M_{n \times d}$, without any degenerate positive singular values, and any embedding dimension $r \in \mathbb{N}$, the loss of the MDS estimator is:*

$$L(\hat{X}^r | \mathbf{x}) \stackrel{a.s.}{=} \sum_{i=1}^r L_{TSVD}(x_i, y(x_i)) \quad (36)$$

$$\text{where } L_{TSVD}(y(x_i), x_i) = \begin{cases} y(x_i)^2 + x_i^2 - 2 \cdot x_i \cdot y(x_i) \cdot c(x_i) & i \leq \min(t, r) \\ \sigma^2 \cdot (1 + \sqrt{\beta})^2 \cdot 1_{[i \leq r]} + x_i^2 \cdot 1_{[i \leq d]} & \text{otherwise} \end{cases}$$

, and $t = \#\{i \in [d] \text{ s.t. } x_i/\sigma > \beta^{\frac{1}{4}}\}$.

Proof. As seen in section 2.6, the TSVD and the MDS embedding would result in the same similarity distance from any matrix. The loss of the TSVD algorithm embedding into r dimensions over some specific n is

$$\begin{aligned} M_n^2(\hat{X}^r, X_n) &= \min_{R \in O(p)} \left\| \sum_{i=1}^r y_{n,i} q_{n,i} \cdot \mathbf{u}_{n,i} \cdot \mathbf{e}_i^\top \cdot R - \sum_{j=1}^d x_j \cdot \mathbf{v}_{n,j} \cdot \begin{bmatrix} \tilde{\mathbf{v}}_{n,j} \\ \mathbf{0}_{p-d} \end{bmatrix}^\top \right\|_F^2 \\ &= \min_{R \in O(p)} \left(\sum_{i=1}^d x_{n,i}^2 + \sum_{j=1}^r y_{n,i}^2 \right) \\ &\quad - 2 \cdot \sum_{i=1}^r \sum_{j=1}^d x_j \cdot y_i \cdot q_{n,i} \cdot \langle \mathbf{u}_{n,i}, \mathbf{v}_{n,j} \rangle \left\langle R^\top \cdot \mathbf{e}_i, \begin{bmatrix} \tilde{\mathbf{v}}_{n,j} \\ \mathbf{0}_{p-d} \end{bmatrix} \right\rangle \end{aligned}$$

where $e_i \in \mathbb{R}^{p_n}$ and $q_{n,i} \in \{\pm 1\}$ for any i and n . The loss of the TSVD algorithm with an embedding dimension of r considers an asymptotic configuration where $n, p \rightarrow \infty$. Following lemma 6

$$\begin{aligned} L(\hat{X}^{TSVD} | \mathbf{x}) &= \lim_{n \rightarrow \infty} M_n^2(\hat{X}^{TSVD}, X_n) \\ &\stackrel{a.s.}{=} \left(\sum_{i=1}^d x_i^2 \right) + \left(\sum_{j=1}^r y(x_j)^2 \right) - 2 \cdot \sum_{i=1}^{\min(r,t)} x_i \cdot y(x_i) \cdot c(x_i) \\ &= \left(\sum_{i=1}^{\min(r,t)} x_i^2 + y(x_i)^2 - 2 \cdot x_i \cdot y(x_i) \cdot c(x_i) \right) \\ &\quad + \left(\sum_{i=\min(r,t)+1}^r \sigma^2 \cdot (1 + \sqrt{\beta})^2 \right) + \left(\sum_{i=\min(r,t)+1}^d x_i^2 \right) \end{aligned}$$

where the minimizer in the limit of $n \rightarrow \infty$ is:

$$R_n = \tilde{V}_n^\top \cdot \text{diag}(w_{n,1}, \dots, w_{n,\max(r,d)}, 1, \dots, 1) \quad (37)$$

and $w_{n,i} \equiv q_{n,i} \cdot \text{sign}(\langle u_{n,i}, v_{n,i} \rangle)$ for any n and $i \in \{1, \dots, \max(r, d)\}$. This follows from the fact that $x_i, y(x_i) > 0$ for any n and $i \in \{1, \dots, \min(r, t)\}$, and the fact that $|\langle R^T \cdot e_i, \tilde{v}_{n,i} \rangle| \leq 1$ for any n and i and for any $R \in O(p_n)$.

□

Lemma 9. *Given the same formulation as in the previous lemma 8. The explicit function of L_{TSVD} for any $i \leq \min(t, r)$ is:*

$$L_{TSVD}(y(x_i), x_i) = \left(\sqrt{x_i^2 + \sigma^2} - \sqrt{\frac{x_i^4 - \beta \cdot \sigma^4}{x_i^2}} \right)^2 + \frac{2 \cdot \beta \cdot \sigma^4}{x_i^2} + \beta \cdot \sigma^2 \quad (38)$$

Proof. Following lemma 6 and lemma 8, we can derive (38):

$$\begin{aligned} L_{TSVD}(x, y(x)) &= x^2 + y(x)^2 - 2 \cdot x \cdot y(x) \cdot c(x) \\ &= x^2 + \sigma^2 \cdot \left((x/\sigma + \frac{1}{x/\sigma}) \cdot (x/\sigma + \frac{\beta}{x/\sigma}) \right) \\ &\quad - 2 \cdot x \cdot \sigma \cdot \sqrt{(x/\sigma + \frac{1}{x/\sigma})(x/\sigma + \frac{\beta}{x/\sigma})} \cdot \sqrt{\frac{(x/\sigma)^4 - \beta}{(x/\sigma)^4 + \beta \cdot (x/\sigma)^2}} \\ &= 2 \cdot x^2 + \sigma^2 + \beta \cdot \sigma^2 + \frac{\beta \cdot \sigma^4}{x^2} \\ &\quad - 2 \cdot \sigma^2 \cdot \sqrt{((x/\sigma)^2 + 1)((x/\sigma)^2 + \beta)} \cdot \sqrt{\frac{(x/\sigma)^4 - \beta}{(x/\sigma)^2 \cdot ((x/\sigma)^2 + \beta)}} \\ &= 2 \cdot x^2 + \sigma^2 + \beta \cdot \sigma^2 + \frac{\beta \cdot \sigma^4}{x^2} - 2 \cdot \sigma^2 \cdot \sqrt{\frac{((x/\sigma)^2 + 1) \cdot ((x/\sigma)^4 - \beta)}{(x/\sigma)^2}} \\ &= 2 \cdot x^2 + \sigma^2 + \beta \cdot \sigma^2 + \frac{\beta \cdot \sigma^4}{x^2} - 2 \cdot \sqrt{\frac{(x^2 + \sigma^2) \cdot (x^4 - \beta \cdot \sigma^4)}{x^2}} \\ &= x^2 + \sigma^2 \cdot \left((x/\sigma + \frac{1}{x/\sigma}) \cdot (x/\sigma + \frac{\beta}{x/\sigma}) \right) \\ &\quad - 2 \cdot x \cdot \sigma \cdot \sqrt{(x/\sigma + \frac{1}{x/\sigma})(x/\sigma + \frac{\beta}{x/\sigma})} \cdot \sqrt{\frac{(x/\sigma)^4 - \beta}{(x/\sigma)^4 + \beta \cdot (x/\sigma)^2}} \\ &= 2 \cdot x^2 + \sigma^2 + \beta \cdot \sigma^2 + \frac{\beta \cdot \sigma^4}{x^2} \\ &\quad - 2 \cdot \sigma^2 \cdot \sqrt{((x/\sigma)^2 + 1)((x/\sigma)^2 + \beta)} \cdot \sqrt{\frac{(x/\sigma)^4 - \beta}{(x/\sigma)^2 \cdot ((x/\sigma)^2 + \beta)}} \\ &= 2 \cdot x^2 + \sigma^2 + \beta \cdot \sigma^2 + \frac{\beta \cdot \sigma^4}{x^2} \\ &\quad - 2 \cdot \sigma^2 \cdot \sqrt{\frac{((x/\sigma)^2 + 1) \cdot ((x/\sigma)^4 - \beta)}{(x/\sigma)^2}} \end{aligned}$$

$$\begin{aligned}
&= 2 \cdot x^2 + \sigma^2 + \beta \cdot \sigma^2 + \frac{\beta \cdot \sigma^4}{x^2} - 2 \cdot \sqrt{\frac{(x^2 + \sigma^2) \cdot (x^4 - \beta \cdot \sigma^4)}{x^2}} \\
&= x^2 + \sigma^2 + \frac{x^4 - \beta \cdot \sigma^4}{x^2} + \beta \cdot \sigma^2 + \frac{2 \cdot \beta \cdot \sigma^4}{x^2} \\
&\quad - 2 \cdot \sqrt{\frac{(x^2 + \sigma^2) \cdot (x^4 - \beta \cdot \sigma^4)}{x^2}} \\
&= \left(\sqrt{x^2 + \sigma^2} - \sqrt{\frac{x^4 - \beta \cdot \sigma^4}{x^2}} \right)^2 + \beta \cdot \sigma^2 + \frac{2 \cdot \beta \cdot \sigma^4}{x^2}
\end{aligned}$$

□

Proof of Theorem 1. The result now follows from Lemma 8 and Lemma 9. □

5.5. Optimal SVHT Asymptotic Loss

Lemma 10. Let $d \in \mathbb{N}$. For any matrix $X \in M_{n \times d}$, without any degenerate positive singular values, and any monotone increasing shrinker $\eta : \mathbb{R} \rightarrow \mathbb{R}$, which holds $\eta(y) = 0$ for any $y \leq \sigma \cdot (1 + \sqrt{\beta})$, the η estimator has the following loss:

$$L(\hat{X}^\eta | x) \stackrel{a.s.}{=} \sum_{i=1}^n L_\eta(\eta(y(x_i)), x_i) \quad (39)$$

where $L_\eta(\hat{x}_i, x_i) = \begin{cases} \hat{x}_i^2 + x_i^2 - 2 \cdot x_i \cdot \hat{x}_i \cdot c(x_i) & \text{if } x_i > \sigma \cdot \beta^{1/4} \\ x_i^2 \cdot 1_{[i \leq d]} & \text{otherwise} \end{cases}$
and $t = \#\{i \in [d] : x_i > \sigma \cdot \beta^{1/4}\}$.

Proof. The loss of any monotone increasing shrinker, as discussed in subsection 2.6, over some specific n is

$$\begin{aligned}
M_n^2(\hat{X}^\eta, X_n) &= \min_{R \in O(p_n)} \left\| \sum_{i=1}^t \eta(y_{n,i}) \cdot q_{n,i} \cdot \mathbf{u}_{n,i} \cdot \mathbf{e}_i^\top \cdot R - \sum_{j=1}^d x_j \cdot \mathbf{v}_{n,j} \cdot \tilde{\mathbf{v}}_{n,j}^\top \right\|_F^2 \\
&= \min_{R \in O(p_n)} \left(\sum_{i=1}^d x_i^2 \right) + \left(\sum_{j=1}^t \eta(y_{n,j}) \right)^2 \\
&\quad - 2 \cdot \sum_{i=1}^t \sum_{j=1}^d x_j \cdot \eta(y_{n,i}) \cdot q_{n,i} \cdot \langle \mathbf{u}_{n,i}, \mathbf{v}_{n,j} \rangle \langle R^\top \cdot \mathbf{e}_i, \tilde{\mathbf{v}}_{n,j} \rangle
\end{aligned}$$

where $e_i \in \mathbb{R}^{p_n}$ and $q_{n,i} \in \{\pm 1\}$ for any n and i . By using the same derivation as in lemma 8 and assuming that η is a monotone increasing function, we get

$$\begin{aligned}
L(\hat{X}^\eta | \mathbf{x}) &= \lim_{n \rightarrow \infty} M_n^2(\hat{X}^\eta, X_n) \\
&\stackrel{a.s.}{=} \left(\sum_{i=1}^t \eta(y(x_i))^2 + x_i^2 - 2 \cdot x_i \cdot \eta(y(x_i)) \cdot c(x_i) \right) + \sum_{j=t+1}^d x_j^2
\end{aligned}$$

where the minimizer R is the same as in 8. □

The following Lemma is elementary:

Lemma 11. Given a function $f : \mathbb{R} \rightarrow \mathbb{R}$, which has the following properties:

1. It is a 3rd degree polynomial, with three real roots.
2. $\lim_{x \rightarrow s \cdot \infty} f(x) = -s \cdot \infty$ for any $s \in \{\pm 1\}$
3. It has exactly two real critical points ($\frac{\partial f}{\partial x} = 0$), where

Then $f(a) < 0 < f(b)$ and there exists a single root of f in each of the following domains: $(-\infty, a)$, (a, b) , (b, ∞)

We are now ready to prove our next main result.

Proof of Theorem 2. Following lemma 10, the optimal SVHT estimator should minimize $L_\eta(y(x), x)$. As we consider the threshold estimators we would like to find when $L_\eta(y(x), x) \leq L_\eta(0, x)$, for any $y(x) \geq \sigma \cdot \beta^{1/4}$

$$\begin{aligned} y(x)^2 + x^2 - 2 \cdot x \cdot y(x) \cdot c(x) &\leq x^2 \\ y(x) - 2 \cdot x \cdot c(x) &\leq 0 \end{aligned}$$

Following lemma 6, the following properties should hold $x \geq \sigma \cdot \beta^{1/4}$ and $c(x) \geq 0$. By plugging-in their definitions we get

$$\begin{aligned} 0 &\geq \sigma \cdot \sqrt{\left(x/\sigma + \frac{1}{x/\sigma}\right)\left(x/\sigma + \frac{\beta}{x/\sigma}\right)} - 2 \cdot x \cdot \sqrt{\frac{(x/\sigma)^4 - \beta}{(x/\sigma)^4 + \beta \cdot (x/\sigma)^2}} \\ &= \frac{\sigma}{x/\sigma} \cdot \sqrt{\left((x/\sigma)^2 + 1\right)\left((x/\sigma)^2 + \beta\right)} - 2 \cdot \sigma \cdot \sqrt{\frac{(x/\sigma)^4 - \beta}{(x/\sigma)^2 + \beta}} \\ &= \frac{\sigma}{x/\sigma \cdot \sqrt{(x/\sigma)^2 + \beta}} \left(\left((x/\sigma)^2 + \beta \right) \sqrt{(x/\sigma)^2 + 1} - 2(x/\sigma) \sqrt{(x/\sigma)^4 - \beta} \right) \end{aligned}$$

Implying

$$0 \geq \left((x/\sigma)^2 + \beta \right)^2 \left((x/\sigma)^2 + 1 \right) - 4(x/\sigma)^2 \left((x/\sigma)^4 - \beta \right)$$

or equivalently

$$-3 \cdot (x/\sigma)^6 + (x/\sigma)^4 \cdot (1 + 2 \cdot \beta) + (x/\sigma)^2 \cdot (\beta^2 + 6\beta) + \beta^2 \leq 0. \quad (40)$$

We would like to show that there exists a unique threshold value a where for any $x < a$ holds $L_\eta(x, y(x)) \geq L_\eta(x, 0)$ and for any $x > a$ holds $L_\eta(x, y(x)) \leq L_\eta(x, 0)$.

In order to show that there exists exactly one real positive solution we define: $z \equiv (x/\sigma)^2$, and we would like to show that:

$$f(z) = -3 \cdot z^3 + (2\beta + 1) \cdot z^2 + (\beta^2 + 6 \cdot \beta) \cdot z + \beta^2 \quad (41)$$

has only one real positive root.

$f(z)$ has three real distinct roots, since its Discriminant is positive-

$$\begin{aligned}
\Delta_3 &= (2\beta + 1)^2 \cdot (\beta^2 + 6\beta)^2 - 4 \cdot (-3) \cdot (\beta^2 + 6\beta)^3 - 4 \cdot (2\beta + 1)^3 \cdot (\beta^2) \\
&- 27 \cdot (-3)^2 \cdot (\beta^2)^2 + 18 \cdot (-3) \cdot (2\beta + 1) \cdot (\beta^2 + 6\beta) \cdot \beta^2 \\
&= \beta^2 \cdot ((4\beta^2 + 4\beta + 1) \cdot (\beta^2 + 12\beta + 36) + 12 \cdot \beta(\beta^3 + 18\beta^2 + 108\beta + 216) \\
&- 4 \cdot (8\beta^3 + 12\beta^2 + 6\beta + 1) - 243\beta^2 - 54 \cdot (2\beta^3 + 13\beta^2 + 6\beta)) \\
&= \beta^2 \cdot ((4\beta^4 + 52\beta^3 + 193\beta^2 + 156\beta + 36) + (12\beta^4 + 216\beta^3 + 1296\beta^2 + 2592\beta) \\
&- (32\beta^3 + 48\beta^2 + 24\beta + 4) - 243\beta^2 - (108\beta^3 + 702\beta^2 + 324\beta)) \\
&= \beta^2 \cdot (16\beta^4 + 128\beta^3 + 496\beta^2 + 2400\beta + 32) \\
&> 0
\end{aligned}$$

where $\beta \in (0, 1]$. Now, we would like to show that only one root is positive. Therefore we start by finding the extreme point of the function-

$$0 = \frac{\partial f(z)}{z} = -9 \cdot z^2 + 2(2 \cdot \beta + 1) \cdot z + \beta^2 + 6 \cdot \beta$$

Its roots are

$$z_{1,2} = \frac{2 \cdot \beta + 1 \pm \sqrt{(2 \cdot \beta + 1)^2 + 9(\beta^2 + 6 \cdot \beta)}}{9}$$

We can see that $z_1 < 0 < z_2$. Using lemma 11 we can deduce that $f(z_1) < 0 < f(z_2)$.

Moreover, following the lemma we know that there exists only one root in the domain of (z_1, z_2) . Since $f(0) = \beta^2$, the root is located in $(z_1, 0)$, meaning that f contains only one positive root.

Now, if we describe $f(z)$ using x instead of z , then the function would have six roots - one strictly positive, one strictly negative and four complex. Moreover, the value of f between zero and the positive root would be strictly positive, while after that point it would become strictly negative. Meaning that there exists a unique threshold that minimizes $L_\eta(\eta(y(x)), x)$ over any x , where $\eta(y) = y \cdot 1_{[a < y]}$.

Now will show that the real positive root is bigger than $\sigma \cdot \beta^{1/4}$, by showing that $z_2 > \beta^{1/2}$ since z_2 is smaller than the positive root

$$\begin{aligned}
\frac{2 \cdot \beta + 1 + \sqrt{(2 \cdot \beta + 1)^2 + 9(\beta^2 + 6 \cdot \beta)}}{9} &> \beta^{1/2} \\
2 \cdot \beta + 1 + \sqrt{(2 \cdot \beta + 1)^2 + 9(\beta^2 + 6 \cdot \beta)} &> 9 \cdot \beta^{1/2} \\
\sqrt{(2 \cdot \beta + 1)^2 + 9(\beta^2 + 6 \cdot \beta)} &> 9 \cdot \beta^{1/2} - 2 \cdot \beta - 1
\end{aligned}$$

The LHS is strictly positive while the RHS of the equation has two roots $\beta = \frac{(9 \pm \sqrt{73})^2}{16}$. Meaning that we need to validate the inequality over the following domains $\beta \in (0, \frac{(9 - \sqrt{73})^2}{16})$ and $(\frac{(9 - \sqrt{73})^2}{16}, 1]$ as we only consider $\beta \in (0, 1]$. The RHS is continuous over $\beta \in (0, 1]$, meaning that by sampling a single point in each of the domains we can see that it is negative in $(0, \frac{(9 - \sqrt{73})^2}{16})$, and positive in the second domain. Meaning that the inequality holds for any $\beta \in (0, \frac{(9 - \sqrt{73})^2}{16}]$.

As for the second domain, both sides of the inequality are positive meaning that we can take a square of each of the sides while keeping the inequality:

$$\begin{aligned} (2 \cdot \beta + 1)^2 + 9(\beta^2 + 6 \cdot \beta) &> (9 \cdot \beta^{1/2} - 2 \cdot \beta - 1)^2 \\ 13 \cdot \beta^2 + 58 \cdot \beta + 1 &> 81 \cdot \beta + 4 \cdot \beta^2 + 1 - 36 \cdot \beta^{3/2} + 4 \cdot \beta - 18 \cdot \beta^{1/2} \\ 9 \cdot \beta^2 + 36 \cdot \beta^{3/2} - 27 \cdot \beta + 18 \cdot \beta^{1/2} &> 0 \end{aligned}$$

It is positive since

$$\begin{aligned} 36 \cdot \beta^{3/2} - 27 \cdot \beta + 18 \cdot \beta^{1/2} &= 9 \cdot \beta^{1/2}(4 \cdot \beta - 3 \cdot \beta^{1/2} + 2) \\ &= 9 \cdot \beta^{1/2} \left((2 \cdot \beta^{1/2} - \frac{3}{4})^2 - \frac{9}{16} + 2 \right) \\ &> 0 \end{aligned}$$

Following lemma 6 the threshold should be strictly bigger then $\lambda > \sigma \cdot (1 + \sqrt{\beta})$ when applied on the noisy singular values. □

5.6. Optimal Continuous Shrinker Asymptotic Loss

Proof of Theorem 3. Following lemma 10, the optimal continuous shrinker should minimize $L_\eta(\eta(y(x)), x)$ for $y \geq \sigma \cdot (1 + \sqrt{\beta})$

$$L_\eta(\eta(y(x)), x) = \eta(y(x))^2 + x^2 - 2 \cdot x \cdot \eta(y(x)) \cdot c(x)$$

while for $y < \sigma \cdot (1 + \sqrt{\beta})$ it should hold $\eta(y) = 0$. Now since L_η is convex in $\eta(y(x))$ the optimal shrinker satisfies

$$0 = \frac{\partial}{\partial \eta(y(x))} (L_\eta(\eta(y(x)), x)) = 2 \cdot \eta(y(x)) - 2 \cdot x \cdot c(x)$$

meaning that

$$\eta^*(y(x)) = x \cdot c(x). \tag{42}$$

Following lemma 6 $x \geq \sigma \cdot \beta^{1/4}$ and $c(x) \geq 0$. Next we plug-in the definitions of $y(x)$ and $c(x)$

$$\begin{aligned}
\eta^*(y(x)) &= x \cdot \sqrt{\frac{(x/\sigma)^4 - \beta}{(x/\sigma)^4 + \beta \cdot (x/\sigma)^2}} \\
&= \sigma \cdot \sqrt{\frac{(x/\sigma)^4 - \beta}{(x/\sigma)^2 + \beta}} \\
&= \sqrt{\frac{x^4 - \beta \cdot \sigma^4}{x^2 + \beta \cdot \sigma^2}} \\
&= \sqrt{x^2 - \frac{x^2 \cdot \beta \cdot \sigma^2 + \beta \cdot \sigma^4}{x^2 + \beta \cdot \sigma^2}} \\
&= \sqrt{x^2 - \beta \cdot \sigma^2 \frac{x^2 + \sigma^2}{x^2 + \beta \cdot \sigma^2}} \\
&= \sqrt{x^2 - \beta \cdot \sigma^2 \cdot \left(1 + \frac{\sigma^2 \cdot (1 - \beta)}{x^2 + \beta \cdot \sigma^2}\right)} \\
&= \sqrt{x^2 - \beta \cdot \sigma^2 - \frac{\sigma^4 \cdot \beta \cdot (1 - \beta)}{x^2 + \beta \cdot \sigma^2}} \\
&= \sigma \cdot \sqrt{(x/\sigma)^2 - \beta - \frac{\beta(1 - \beta)}{(\frac{x}{\sigma})^2 + \beta}}
\end{aligned} \tag{43}$$

$\eta^*(y(x))$ is continuous at $x = \sigma \cdot \beta^{1/4}$ since

$$\begin{aligned}
\lim_{x \rightarrow (\sigma \cdot \beta^{1/4})^-} \eta_{opt}(y(x)) &= 0 \\
\lim_{x \rightarrow (\sigma \cdot \beta^{1/4})^+} \eta_{opt}(y(x)) &= \sqrt{\frac{0}{x^2 + \beta \cdot \sigma^2}} = 0
\end{aligned}$$

Meaning that this optimal shrinker is indeed continuous. □

Proof of Theorem 4. Following lemma 10 and (42), the loss could be expressed as follows

$$\begin{aligned}
L(\hat{X}^{\eta^*} | \mathbf{x}) &\stackrel{\text{a.s.}}{=} \sum_{i=1}^t \eta(y(x_i))^2 + x_i^2 - 2 \cdot x_i \cdot \eta(y(x_i)) \cdot c(x_i) + \sum_{i=t+1}^d x_i^2 \\
&= \sum_{i=1}^t (c(x_i) \cdot x)^2 + x_i^2 - 2 \cdot x_i \cdot (c(x_i) \cdot x_i) \cdot c(x_i) + \sum_{i=t+1}^d x_i^2 \\
&= \sum_{i=1}^t x_i^2 - c(x_i)^2 \cdot x_i^2 + \sum_{i=t+1}^d x_i^2 \\
&= \sum_{i=1}^t x_i^2 \cdot (1 - c(x_i)^2) + \sum_{i=t+1}^d x_i^2 \\
&= \sum_{i=1}^t x_i^2 \cdot \left(1 - \frac{(x_i/\sigma)^4 - \beta}{(x_i/\sigma)^4 + \beta \cdot (x_i/\sigma)^2}\right) + \sum_{i=t+1}^d x_i^2 \\
&= \sum_{i=1}^t x_i^2 \cdot \left(\frac{\beta \cdot (x_i/\sigma)^2 + \beta}{(x_i/\sigma)^4 + \beta \cdot (x_i/\sigma)^2}\right) + \sum_{i=t+1}^d x_i^2 \\
&= \sum_{i=1}^t \beta \cdot \sigma^2 \cdot \frac{(x_i/\sigma)^2 + 1}{(x_i/\sigma)^2 + \beta} + \sum_{i=t+1}^d x_i^2 \\
&= \beta \cdot \sigma^2 \left(\sum_{i=1}^t \frac{1 - \beta}{(x_i/\sigma)^2 + \beta} + 1 \right) + \sum_{i=t+1}^d x_i^2
\end{aligned} \tag{44}$$

□

Lemma 12. Let $r, d \in \mathbb{N}$ and $X \in M_{n \times d}$, without any degenerate positive singular values. Denote $\delta_i \equiv L_{TSVD}(x_i^r, x_i) - L_{\eta}(\eta^*(y(x_i)), x_i)$.

1. if $x_i \in (0, \sigma \cdot \beta^{1/4})$ then

$$\delta_i = 1_{[i \leq r]} \cdot \sigma^2 \cdot (1 + \sqrt{\beta})^2 \tag{45}$$

2. if $x_i \in (\sigma \cdot \beta^{1/4}, \infty]$ and $i > r$ then

$$\delta_i = \sigma^2 \cdot \frac{(x_i/\sigma)^4 - \beta}{(x_i/\sigma)^2 + \beta} \tag{46}$$

3. if $x_i \in (\sigma \cdot \beta^{1/4}, \infty)$ and $i \leq r$ then

$$\delta_i = \left(\sqrt{x_i^2 + \sigma^2} - \sqrt{\frac{x_i^4 - \beta \cdot \sigma^4}{x_i^2}} \right)^2 + \beta \cdot \sigma^2 \cdot \frac{(x_i/\sigma)^2 \cdot (1 + \beta) + 2\beta}{(x_i/\sigma)^4 + \beta \cdot (x_i/\sigma)^2} \tag{47}$$

where \hat{x}_i^r is the i -th singular value of the embedding done by the TSVD embedding algorithm \hat{X}^r .

Proof. Following lemma 8, 9,10, and theorem 4 the following domains should be investigated over x_i : $[0, \sigma \cdot \beta^{1/4}]$, $[\sigma \cdot \beta^{1/4}, \infty]$ when $i > r$, and when $i \leq r$.

First we examine the domain of $(0, \sigma \cdot (1 + \sqrt{\beta}))$

$$\begin{aligned}\delta_i &= \sigma^2 \cdot (1 + \sqrt{\beta})^2 \cdot 1_{[i \leq r]} + x_i^2 \cdot 1_{[i \leq d]} - x_i^2 \cdot 1_{[i \leq d]} \\ &= \sigma^2 \cdot (1 + \sqrt{\beta})^2 \cdot 1_{[i \leq r]}\end{aligned}$$

Following equation (44), the difference between the two functions for $x_i \in (\sigma \cdot \beta^{1/4}, \infty)$ when $i > r$ is

$$\begin{aligned}\delta_i &= x_i^2 - x_i^2 \cdot \left(1 - \frac{(x_i/\sigma)^4 - \beta}{(x_i/\sigma)^4 + \beta \cdot (x_i/\sigma)^2}\right) \\ &= \sigma^2 \cdot \frac{(x_i/\sigma)^4 - \beta}{(x_i/\sigma)^2 + \beta}\end{aligned}$$

While when $i \leq r$ it is

$$\begin{aligned}\delta_i &= \left(\left(\sqrt{x_i^2 + \sigma^2} - \sqrt{\frac{x_i^4 - \beta \cdot \sigma^4}{x_i^2}} \right)^2 + \frac{2 \cdot \beta \cdot \sigma^4}{x_i^2} + \beta \cdot \sigma^2 \right) \\ &\quad - \beta \cdot \sigma^2 \cdot \left(\frac{1 - \beta}{(x_i/\sigma)^2 + \beta} + 1 \right) \\ &= \left(\sqrt{x_i^2 + \sigma^2} - \sqrt{\frac{x_i^4 - \beta \cdot \sigma^4}{x_i^2}} \right)^2 + \beta \cdot \sigma^2 \cdot \left(\frac{2}{(x_i/\sigma)^2} - \frac{1 - \beta}{(x_i/\sigma)^2 + \beta} \right) \\ &= \left(\sqrt{x_i^2 + \sigma^2} - \sqrt{\frac{x_i^4 - \beta \cdot \sigma^4}{x_i^2}} \right)^2 \\ &\quad + \beta \cdot \sigma^2 \cdot \frac{(x_i/\sigma)^2 \cdot (1 + \beta) + 2\beta}{(x_i/\sigma)^4 + \beta \cdot (x_i/\sigma)^2}\end{aligned}$$

□

Proof of Theorem 5. The result follows from Lemma 8, Lemma 10 and Lemma 12. □

Proof of Theorem 6. Denote the singular values of $H \cdot Y_n$ by $y_{1,n} \geq y_{n,n} \geq 0$. A similarity matrix S_n is defined through it corresponding Δ_n , as shown in (1). Denote S_n 's eigenvalues by $s_{n,1} \geq s_{n,n} \geq 0$. Theorem 7 assembles the following connection $S_n = (H \cdot Y_n) \cdot (H \cdot Y_n)^\top$. As a consequence, $s_{n,i} = y_{n,i}^2$ holds.

Let F_n be the Cumulative Empirical Spectral Distribution of S_n , and let $Median(\cdot)$ be the functional that extracts the median out of any Cumulative distribution function.

$$Median(F_n) = y_{n,med}$$

By Lemma 6, all but the d largest singular values $\{y_i\}$ asymptotically follow the Quarter Circle distribution (30) as $n \rightarrow \infty$. Therefore the eigenvalues of S act as the Marcenko Pastur

distribution [38].

We denote the Cumulative Empirical Spectral Distribution of S/σ^2 by \tilde{F}_n , making the effective noise level on it to be 1. Under our asymptotic framework, almost surely, \tilde{F}_n converges weakly to a limiting distribution, F_{MP} , the CDF of the Marceno Pastur distribution with shape parameter β [39]. The median functional is continuous for weak convergence at F_{MP} , therefore

$$\lim_{n \rightarrow \infty} \frac{S_{n,med}}{\sigma^2} = \lim_{n \rightarrow \infty} \text{Median}(\tilde{F}_n) \stackrel{a.s.}{=} \text{Median}(F_{MP}) = \mu_\beta$$

By that we can conclude the almost surely convergence of our estimator

$$\lim_{n \rightarrow \infty} \hat{\sigma}^2(S_n) = \lim_{n \rightarrow \infty} \frac{S_{n,med}}{\mu_\beta} \stackrel{a.s.}{\rightarrow} \sigma^2 \quad (48)$$

□

6. Conclusion

This paper presents a systematic treatment of Multidimensional Scaling (MDS) from a decision-theoretic perspective. By introducing a loss function which measures the embedding accuracy, and introducing a useful asymptotic model we were able to derive an asymptotically precise selection rule for the embedding dimension, as well as a new version of MDS which uses an optimal shrinkage non-linearity, under the assumption of white measurement noise. The proposed algorithm is no more complicated to implement than classical MDS, yet offers significant improvement in performance as measured by the asymptotic loss. Our results indicate that manifold learning algorithms are inherently sensitive to ambient noise in high dimensions, a phenomenon that calls for further study.

Acknowledgements

The authors thank Zohar Yachini and Shay Ben Elazar for fascinating discussions on applications of MDS. This work was partially supported by H-CSRC Security Research Center, Israeli Science Foundation grant no. 1523/16 and German-Israeli foundation for scientific research and development (GIF) Program no. I-1100-407.1-2015.

Appendix: The case $\beta > 1$

Surprisingly we can see that all of our results admit the case of $\beta \geq 1$ as well. We give a sketch the proof of lemma 13 that is the basis for analyzing the loss function under the new β domain. Moreover, we show that the optimal threshold is still bigger than the bulk edge ($\sigma \cdot (1 + \sqrt{\beta})$). We finish by showing how one should find σ .

One important feature under this configuration is that $\text{rank}(S) = p$, meaning that the algorithm can infer the ambient dimension of the data under this configuration from the distance matrix Δ .

Lemma 13 (Variation of Lemma 6).

1.

$$\lim_{n \rightarrow \infty} y_{n,i} \stackrel{a.s.}{=} \begin{cases} y(x) & \text{if } i \in [t] \\ \sigma \cdot (1 + \sqrt{\beta}) & \text{otherwise} \end{cases} \quad (.1)$$

2.

$$\lim_{n \rightarrow \infty} |\langle \mathbf{u}_{n,i}, \mathbf{v}_{n,j} \rangle| \stackrel{a.s.}{=} \begin{cases} c(x) & i \in [t] \\ 0 & \text{otherwise} \end{cases} \quad (.2)$$

where $t \equiv \#\{i \in [d] : x_i/\sigma > \beta^{1/4}\}$

Proof. In order to follow lemma 6's proof, one should make some adaptations. Denote $\tilde{X}_n \equiv X_n^\top$ and $\tilde{Y}_n \equiv Y_n^\top$, meaning

$$\tilde{Y}_n = R_n^\top \begin{bmatrix} \tilde{X}_n \\ \mathbf{0}_{(p_n-d) \times n} \end{bmatrix} + Z_n^\top$$

Denote its aspect ratio $\tilde{\beta} \equiv \frac{1}{\beta} = \frac{p_n}{n-1}$ and its effective level $\tilde{\sigma} \equiv \sigma/\sqrt{\beta}$. Denote the new noise matrix by $\tilde{Z}_n \equiv Z_n^\top$. The entries of Z_n are i.i.d distributed and drawn from a distribution with zero mean, variance $\tilde{\sigma}/\sqrt{n-1} = \sigma/\sqrt{p_n}$ and finite fourth moment. As one can suspect the new notations admit the asymptotic model framework that was stated in subsection 2.5. Combining all those notation together, the framework could be written as

$$\tilde{Y}_n = R_n^\top \begin{bmatrix} \tilde{X}_n \\ \mathbf{0}_{(p_n-d) \times n} \end{bmatrix} + \tilde{Z}_n$$

with the aspect ratio $\tilde{\beta} \in (0, 1]$.

Now, by following carefully after the proof of lemma 6. □

Proof of the SVHT. Up until the point where we show that the threshold is bigger then $\sigma \cdot \beta^{1/4}$, the proof is identical. For the this point we show

$$\begin{aligned} \frac{2 \cdot \beta + 1 + \sqrt{(2 \cdot \beta + 1)^2 + 9(\beta^2 + 6 \cdot \beta)}}{9} &> \beta^{1/2} \\ 2 \cdot \beta + 1 + \sqrt{(2 \cdot \beta + 1)^2 + 9(\beta^2 + 6 \cdot \beta)} &> 9 \cdot \beta^{1/2} \\ \sqrt{(2 \cdot \beta + 1)^2 + 9(\beta^2 + 6 \cdot \beta)} &> 9 \cdot \beta^{1/2} - 2 \cdot \beta - 1 \end{aligned}$$

The LHS is strictly positive while the RHS of the equation has two roots $\beta = \frac{(9 \pm \sqrt{73})^2}{16}$. Meaning that we need to validate the inequality over the following domains $\beta \in [1, \frac{(9 + \sqrt{73})^2}{16})$ and $[\frac{(9 + \sqrt{73})^2}{16}, \infty)$ as we only consider $\beta \in [1, \infty)$. The RHS is continuous over $\beta \in [1, \infty)$, meaning that by sampling a single point in each of the domains we can see that it is positive in $[1, \frac{(9 + \sqrt{73})^2}{16})$, and negative in the second domain. Meaning that the inequality holds for any $\beta \in [\frac{(9 + \sqrt{73})^2}{16}, \infty)$.

As for the first domain, both sides of the inequality are positive meaning that we can take a square of each of the sides while keeping the inequality:

$$\begin{aligned} (2 \cdot \beta + 1)^2 + 9(\beta^2 + 6 \cdot \beta) &> (9 \cdot \beta^{1/2} - 2 \cdot \beta - 1)^2 \\ 13 \cdot \beta^2 + 58 \cdot \beta + 1 &> 81 \cdot \beta + 4 \cdot \beta^2 + 1 - 36 \cdot \beta^{3/2} + 4 \cdot \beta - 18 \cdot \beta^{1/2} \\ 9 \cdot \beta^2 + 36 \cdot \beta^{3/2} - 27 \cdot \beta + 18 \cdot \beta^{1/2} &> 0 \end{aligned}$$

39

It is positive since

$$\begin{aligned}
36 \cdot \beta^{3/2} - 27 \cdot \beta + 18 \cdot \beta^{1/2} &= 9 \cdot \beta^{1/2}(4 \cdot \beta - 3 \cdot \beta^{1/2} + 2) \\
&= 9 \cdot \beta^{1/2} \left((2 \cdot \beta^{1/2} - \frac{3}{4})^2 - \frac{9}{16} + 2 \right) \\
&> 0
\end{aligned}$$

Following lemma 13 the threshold should be strictly bigger then $\lambda > \sigma \cdot (1 + \sqrt{\beta})$ when applied on the noisy singular values.

□

Theorem 9 (Variation of Theorem 6). *Consider*

$$\hat{\sigma}(S) = \sqrt{\frac{s_{med}}{\mu_{1/\beta} \cdot \beta}} \quad (.3)$$

where $s_1 \geq \dots \geq s_{\min(n,p)} \geq 0$ are the eigenvalues of S , and s_{med} is their median. Denote the median of the quarter circle distribution [39] for β by μ_β . Then $\hat{\sigma}^2(S_n) \xrightarrow{a.s.} \sigma^2$ as $n \rightarrow \infty$.

References

- [1] Joshua Tenenbaum, Vin De Silva, and John Langford. A global geometric framework for nonlinear dimensionality reduction. *Science*, 290(5500):2319–2323, 2000.
- [2] Sam Roweis and Lawrence Saul. Nonlinear dimensionality reduction by locally linear embedding. *Science*, 290(5500):2323–2326, 2000.
- [3] Ronald R Coifman and Stéphane Lafon. Diffusion maps. *Applied and computational harmonic analysis*, 21(1):5–30, 2006.
- [4] Pascal Vincent, Hugo Larochelle, Yoshua Bengio, and Pierre-Antoine Manzagol. Extracting and composing robust features with denoising autoencoders. pages 1096–1103, 2008.
- [5] Christopher M Bishop, Markus Svensén, and Christopher KI Williams. Developments of the generative topographic mapping. *Neurocomputing*, 21(1):203–224, 1998.
- [6] Aurélien Bellet, Amaury Habrard, and Marc Sebban. A survey on metric learning for feature vectors and structured data. *arXiv preprint arXiv:1306.6709*, 2013.
- [7] Yoshua Bengio, Aaron Courville, and Pascal Vincent. Representation learning: A review and new perspectives. *IEEE transactions on pattern analysis and machine intelligence*, 35(8):1798–1828, 2013.
- [8] WS Torgerson. Multidimensional Scaling: I. Theory and methods. *Psychometrika*, 17(4):401–419, 1952.
- [9] Warren S Torgerson. Theory and methods of scaling. 1958.
- [10] Joseph B Kruskal and Myron Wish. *Multidimensional scaling*, volume 11. Sage, 1978.
- [11] Trevor Cox and Michael Cox. *Multidimensional scaling*. CRC press, 2000.
- [12] Ingwer Borg and Patrick JF Groenen. *Modern multidimensional scaling: Theory and applications*. Springer Science & Business Media, 2005.
- [13] Forrest W Young. *Multidimensional scaling: History, theory, and applications*. Psychology Press, 2013.
- [14] Michael C Hout, Megan H Papesh, and Stephen D Goldinger. Multidimensional scaling. *Wiley Interdisciplinary Reviews: Cognitive Science*, 4(1):93–103, 2013.
- [15] Raymond B. Cattell. The scree test for the number of factors. *Multivariate Behavioral Research*, 1(2):245–276, 1966.
- [16] Erez Peterfreund. Code Supplement for “Multidimensional Scaling of Noisy High Dimensional Data”. Available at <https://purl.stanford.edu/kh576pt3021>.
- [17] Debashis Paul. Asymptotics of sample eigenstructure for a large dimensional spiked covariance model. *Statistica Sinica*, 17(4):1617–1642, 2007.
- [18] Jinho Baik, Gérard Ben Arous, and Sandrine Péché. Phase transition of the largest eigenvalue for nonnull complex sample covariance matrices. *The Annals of Probability*, 33(5):1643–1697, sep 2005.

- [19] David L. Donoho, Matan Gavish, and Iain M. Johnstone. Optimal shrinkage of eigenvalues in the spiked covariance model. *arXiv:1311.0851*, 2013.
- [20] LeCun Yann, Cortes Corinna, and Burges Christopher. THE MNIST DATABASE of handwritten digits. *The Courant Institute of Mathematical Sciences*, pages 1–10, 1998.
- [21] Hideki Tanizawa, Osamu Iwasaki, Atsunari Tanaka, Joseph R Capizzi, Priyankara Wickramasinghe, Mihee Lee, Zhiyan Fu, and Ken-ichi Noma. Mapping of long-range associations throughout the fission yeast genome reveals global genome organization linked to transcriptional regulation. *Nucleic acids research*, 38(22):8164–8177, 2010.
- [22] Gale Young and Alston S Householder. Discussion of a set of points in terms of their mutual distances. *Psychometrika*, 3(1):19–22, 1938.
- [23] John C Gower. Some distance properties of latent root and vector methods used in multivariate analysis. *Biometrika*, 53(3-4):325–338, 1966.
- [24] Trevor Cox and Michael Cox. *Multidimensional scaling*. CRC press, 2000.
- [25] Joseph B Kruskal. Multidimensional scaling by optimizing goodness of fit to a nonmetric hypothesis. *Psychometrika*, 29(1):1–27, 1964.
- [26] J. B. Kruskal. Nonmetric multidimensional scaling: A numerical method. *Psychometrika*, 29(2):115–129, 1964.
- [27] Mitchell AA Cox and Trevor F Cox. Interpreting stress in multidimensional scaling. *Journal of Statistical Computation and Simulation*, 37(3-4):211–223, 1990.
- [28] Peter J. Forrester. *Log-Gases and Random Matrices*. Princeton University Press, Princeton, NJ, 2010.
- [29] David L. Donoho and Matan Gavish. Minimax Risk of Matrix Denoising by Singular Value Thresholding. *Annals of Statistics*, 42(6):2413–2440, 2014.
- [30] Iain M Johnstone. On the distribution of the largest eigenvalue in principal components analysis. *Annals of statistics*, pages 295–327, 2001.
- [31] Florent Benaych-Georges and Raj Rao Nadakuditi. The singular values and vectors of low rank perturbations of large rectangular random matrices. *Journal of Multivariate Analysis*, 111:120–135, 2012.
- [32] Andrey A. Shabalin and Andrew B. Nobel. Reconstruction of a low-rank matrix in the presence of Gaussian noise. *Journal of Multivariate Analysis*, 118:67–76, 2013.
- [33] David L Donoho and Matan Gavish. The optimal hard threshold for singular values is $4/\sqrt{3}$. *IEEE Transactions on Information Theory*, 60(8):5040–5053, 2014.
- [34] Matan Gavish and David L. Donoho. Optimal Shrinkage of Singular Values. *IEEE Transactions on Information Theory*, 63(4):2137–2152, 2017.
- [35] David L Donoho, Matan Gavish, and Iain M Johnstone. Optimal shrinkage of eigenvalues in the spiked covariance model. *Annals of Statistics*, to appear, 2018.
- [36] Damien Passetier and Jian-Feng Yao. Variance estimation and goodness-of-fit test in a high-dimensional strict factor model. *Submitted to Statist. Sinica, arXiv*, 1308, 2013.
- [37] Shira Kritchman and Boaz Nadler. Non-parametric detection of the number of signals: Hypothesis testing and random matrix theory. *IEEE Transactions on Signal Processing*, 57(10):3930–3941, 2009.
- [38] Vladimir Marcenko and Leonid Pastur. Distribution of eigenvalues for some sets of random matrices. *Mathematics USSR Sbornik*, 1(4):457–483, 1967.
- [39] Zhidong Bai and Jack W Silverstein. *Spectral analysis of large dimensional random matrices*, volume 20. Springer, 2010.
- [40] Yong-Qua Yin, Zhi-Dong Bai, and Pathak R Krishnaiah. On the limit of the largest eigenvalue of the large dimensional sample covariance matrix. *Probability theory and related fields*, 78(4):509–521, 1988.
- [41] ZD Bai and YQ Yin. Limit of the smallest eigenvalue of a large dimensional sample covariance matrix. pages 108–127, 2008.